



Durham E-Theses

Integrated intensity measurements in crystal structure analysis

Raper, E. S.

How to cite:

Raper, E. S. (1968) *Integrated intensity measurements in crystal structure analysis*, Durham theses, Durham University. Available at Durham E-Theses Online: <http://etheses.dur.ac.uk/10015/>

Use policy

The full-text may be used and/or reproduced, and given to third parties in any format or medium, without prior permission or charge, for personal research or study, educational, or not-for-profit purposes provided that:

- a full bibliographic reference is made to the original source
- a [link](#) is made to the metadata record in Durham E-Theses
- the full-text is not changed in any way

The full-text must not be sold in any format or medium without the formal permission of the copyright holders.

Please consult the [full Durham E-Theses policy](#) for further details.

INTEGRATED INTENSITY MEASUREMENTS

IN

CRYSTAL STRUCTURE ANALYSIS

by

E. S. Raper, A.R.I.C.

A thesis submitted for the Degree of Master of Science
in the University of Durham.

August, 1968.



ABSTRACT

Some fundamental aspects of the photographic process are described and the relationship between exposure time and density is discussed.

A review of some of the techniques employed in the measurement of the intensities of X-ray reflections is given. Among the techniques reviewed are; the visual method of estimation, the application of photometric techniques in the measurement of peak and integrated intensities and the application of counters in the direct monitoring of the X-ray beam.

The Joyce-Loebl integrating microdensitometer is described, its function and operation discussed. The instrument has a linear response up to about 1.5 D and the linear response of ILFORD INDUSTRIAL G, a double coated X-ray film, extends to 0.7 D. Ideally the I.D.V. corresponding to the limiting density of 0.7 D should be about 250 units, corresponding to a circular spot of about 0.3 mm diameter. Such a spot would be accommodated with X and Y sweeps of 3. Very large spots should be avoided because of the loss of recording sensitivity at high X sweep values and very small spots should be avoided because of their very narrow I.D.V. range.

A limitation on the use of the instrument is caused by the disparity in linear response between the instrument itself and the double coated film normally used. It is recommended that double coated film be replaced with single coated film for the purposes of the intensity record. The advantage of such a move would be a wider and more accurately measured recording range.

The intensity record used in the crystal structure analysis of 2-thioamidopyridine has been obtained by means of the Joyce-Loebl integrating microdensitometer. The bond lengths and angles obtained from the analysis show good agreement with similar bond lengths and angles in related molecules.

It is concluded that the integrating microdensitometer provides a reliable intensity measurement and suggestions are made which should enable maximum accuracy to be obtained from the instrument in the future.

PREFACE

This thesis describes research carried out mostly in the Chemistry Department of the Rutherford College of Technology, Newcastle upon Tyne.

I wish to express my thanks to the Principal and Governors of the College for the provision of research facilities. Thanks are expressed to Mr. L. H. W. Hallett, Head of the Chemistry Department at Rutherford College, for his continued interest in the work. To Dr. T. C. Downie, Principal Lecturer, and Mr. W. Harrison, Research Student, both of the Chemistry Department Rutherford College of Technology, I wish to express my gratitude for much fruitful discussion and for permission to include the results of research undertaken jointly with them.

Finally, I wish to express my sincere thanks to Dr. H. M. M. Shearer, Senior Lecturer, in the University of Durham for his invaluable advice and guidance during the entire project.

CONTENTS

<u>Abstract</u>	ii
<u>Preface</u>	iv
<u>Chapter One</u>	
<u>The Photographic Process</u>	1
<u>Chapter Two</u>	
<u>The Measurement of Intensities</u>	
2.1 Introduction	5
2.2 Visual Intensity Estimation	7
2.3 Peak Intensity Measurements	8
2.4 Integrated Intensity Methods	10
2.5 Accurate Intensity Measurements by Photographic Methods	17
2.6 Automatic Diffractometry	19
2.7 Comparison of Currently Available Methods	29
<u>Chapter Three</u>	
<u>The Joyce-Loebl Integrating Microdensitometer</u>	
3.1 Function	33
3.2 Principle of Operation	33
3.3 General Description	34
3.4 Operating Procedure	38
3.5 Instrument Evaluation	40
<u>Chapter Four</u>	
<u>A Comparison of Double and Single Coated Film Response</u>	
4.1 Introduction	53
4.2 Experimental	54
4.3 Discussion of Results	56
4.4 Summary	62
<u>Chapter Five</u>	
<u>The Crystal Structure of 2-thioamidopyridine C₆H₇N₂S</u>	
5.1 Introduction	75
5.2 Crystal Data	76
5.3 Data Collection and Intensity Measurements	77

5.4 Structure Analysis	78
5.5 Description and Discussion of the Structure	79
<u>Chapter Six</u>	
<u>Conclusion</u>	86
<u>Appendix I</u>	
<u>The Joyce-Loebl Integrating Microdensitometer Circuit Diagram</u>	88
<u>Appendix II</u>	
<u>Tables of Results</u>	89
<u>Appendix III</u>	
<u>Kodak Data Sheet SC-15</u>	100
<u>References</u>	101

LIST OF FIGURES

<u>Figure 2.1</u>	Intensity Profiles (1)	10
<u>Figure 2.2</u>	Intensity Profiles (2)	14
<u>Figure 2.3</u>	Geiger Counter : Counting Rate Versus Applied Voltage	21
<u>Figure 5</u> (a) and (b)	Bonding in Metal-thiopic Chelates	75
<u>Figure 5.2</u>	Bond Lengths and Angles in 2-thioamidopyridine	85
<u>Figure 5.3</u>	Bond Lengths and Angles in Pyridine	85

CHAPTER ONE

THE PHOTOGRAPHIC PROCESS

THE PHOTOGRAPHIC PROCESS

The photosensitive material of a photographic film is silver bromide containing a few per cent of silver iodide and the photographic emulsion consists of grains of silver bromide suspended in gelatin. It is usual for both sides of the film to be coated with the emulsion and this is the case with Ilford Industrial G X-ray film.

The emulsion is very sensitive to X-ray radiation. It is believed that only one quantum in the X-ray region is necessary to produce a developable silver nucleus. (Morimoto and Uyeda, 1964). As a result of exposure to X-rays some of the silver halide grains are sensitised. When the emulsion is treated with developer these sensitised grains gradually change to metallic silver. The total amount of silver produced depends on the number of sensitised silver halide grains in the emulsion and upon the extent to which the developer is allowed to transform the sensitised grains into metallic silver. The fixing process dissolves the excess silver halide unaffected by the developer and also hardens the gelatin. (Mees, 1952).

It is well known that for emulsions exposed to X-rays the Reciprocity Law is obeyed i.e. that the intensity of a spot is a product of the intensity of the X-ray beam and exposure time.

Thus the amount of developable silver nuclei produced in a fixed time is proportional to the intensity of the X-rays falling upon it. When collecting an intensity record however it is usual to keep the intensity of the X-ray beam constant and vary the exposure time. Thus the recorded intensities are related to exposure time.



2

By photometric methods it is possible to determine the intensity of a reflection i.e. the relative amount of deposited silver, by measuring either the transmission or the absorption of light. Alternatively, the amount of developed silver may be measured by a visual estimate of the intensity of the reflection (Hunter and Driffield, 1890).

Let L_0 = original intensity

L = emergent intensity

$$\text{so Transmission} = \frac{L}{L_0} \quad (1)$$

$$\text{or Opacity} = \frac{L_0}{L} \quad (2)$$

If the transmitted intensity, L , is unity (2) yields $0 = L_0$. Thus 0 may be thought of as the intensity of light which must fall on the film in order that unit intensity emerges through it.

Consider a small thickness dt of developed emulsion containing N silver atoms per unit area. Let light of initial intensity L_0 fall on this small layer. The absorption by the silver reduces the intensity by an amount dL . This reduction is proportional to the amount of silver, to the initial intensity, and to the film thickness i.e.

$$-dL = k N L dt \quad (3)$$

where k is a proportionality constant, the linear absorption coefficient expressed in cm^{-1} units.

Therefore

$$-\frac{dL}{L} = k N dt \quad (4)$$

On integration this gives

$$\ln I_0 - I = k N t$$

$$\text{or } \ln \frac{I_0}{I} = k N t \quad (5)$$

The quantity $k N t$ is proportional to the density of silver in the film.

It is customary to express (5) in terms of common logarithms.

On rewriting, (5) becomes

$$\log_{10} \frac{I_0}{I} = 0.4343 k N t \quad (6)$$

$$\text{or } \log_{10} \frac{I_0}{I} = D \quad (7)$$

since the quantity $0.4343 k N t$ is proportional to the density of silver in the film and is defined as the density D , for photographic purposes.

Thus the density of the precipitated silver can be measured by $\log_{10} (I_0/I)$. This density value will be proportional to X-ray exposure up to some exposure level which corresponds to the limiting density of the film. A summary of the limiting densities of various types of commercially available X-ray film has been made by Morimoto and Uyeda (1964). At density values beyond the limiting density the intensity of the reflection does not increase linearly with increasing exposure. This is due to the absorption of quanta by grains which have already been sensitised. Repeated absorption by the same grain does not increase the number of developable grains.

It has already been pointed out that density is a linear function of exposure up to a limiting density value. Van Horn (1951) has shown how the linear, density : exposure, relation can be extended to higher

densities. This technique couples moderate exposure times with long development times. Increased development times do, however, tend to increase the background density of the film.

CHAPTER TWO

THE MEASUREMENT OF INTENSITIES

THE MEASUREMENT OF INTENSITIES

2.1 Introduction

The electrons in each atom within a crystal are capable of scattering an incident X-ray beam. The scattered radiation is associated with an allowed crystal plane which is identified by its Miller Index triplet, $h k l$. Such scattered rays are called reflections and the intensity of each reflection forms the basic data of X-ray structural analysis.

In the period immediately after Max von Laue's experiments with X-rays (1912), the intensities of X-ray beams diffracted by single crystals were measured with ionisation spectrometers. This technique, developed by W. H., and W. L., Bragg, (1913) involved passing the diffracted beam into an ionisation chamber containing a gas (e.g. SO_2) and measuring the ionisation current on an electroscope. The method was slow, largely because of the great care needed to measure each reflection. However, it did yield results of fundamental importance (Bragg W. H. & W. L., 1915) e.g. it established the ionic nature of sodium chloride by showing the system to consist of 6.6 coordinated sodium and chloride ions. Gradually however the method fell into disuse and it was replaced in the mid-nineteen-twenties by photographic methods. The measurement of intensities from X-ray photographs is based on the principle that the degree of blackening of the photograph is a measure of the intensity of the diffracted beam. The degree of blackening may be estimated visually or an actual intensity measurement may be made instrumentally. For visual intensity estimations, the reflections are usually compared with a standard exposure scale. In this way the intensity of the reflections

are related to relative exposure times. This technique is discussed in more detail in section 2.2.

Two types of intensity measurement are possible from X-ray photographs, namely, peak and integrated intensities. Some aspects of peak intensity measurements are discussed in section 2.3.

Integrated intensities are more difficult to measure than peak intensities. An integrated intensity measurement involves a summation of the individual intensities over the whole area of the reflection. Several photometric techniques have been devised to determine integrated intensities. They utilise the principle of comparing the logarithmic ratio of incident and emergent light beam intensity, $D = \log_{10} \frac{I_0}{I}$, for each individual intensity measurement. Various instrumental techniques may be employed to obtain this ratio and also to sum either all the individual D values for a single reflection or alternatively, to sum $\log I$'s since I_0 will be constant for any one instrument. Several of these methods are compared in section 2.4.

The experimental requirements for accurate intensity measurements from photographic film have been investigated by Jeffrey and his associates (1964). Some aspects of this work are considered in section 2.5.

The search for greater accuracy than can be obtained from photographic methods has led back, at least in principle, to the ionisation spectrometer. An important advance in this respect has been the replacement of the ionisation spectrometer by counting techniques. Proportional or scintillation counters, incorporated in automatic diffractometers, provide a means of determining peak, integrated or absolute intensities

(R. D. Burbank, 1964, 1965). Some aspects of these techniques of intensity measurements are considered in section 2.6.

Finally, an overall assessment of the methods currently employed in intensity determination is made in section 2.7.

2.2 Visual Intensity Estimation

The visual estimation usually involves the preparation of a standard exposure scale, followed by a comparison of the intensities of the reflections on the standard scale with the intensities of the actual X-ray reflections. A standard exposure scale may be prepared by selecting a suitable reflection from the crystal being investigated; this may be achieved by rotating the crystal through a narrow angular range. A series of graded exposures of this one reflection is then recorded on the same piece of film.

Kaan and Cole (1948) have discussed factors which affect the visual estimation of peak intensities. The total error inherent in the visual method is placed by these workers at $\pm 10\%$ of the intensity value. They point out that eye estimation is physically tiring and errors are likely because of variations in size and density gradients between the reflections and spots on the exposure scale. Furthermore, several observers may produce quite different results because the linear dimensions of the reflections are close to the limit of smallest detail visible by eye. Corrections should be made where appropriate to any visually estimated reflection for the increased angle of incidence (Cox and Shaw, 1930, Whittaker, 1953, Bullen, 1953 and Grenville - Wells, 1955). Visual intensities obtained from upper and lower halves of Weissenberg

photographs, from layers other than the zero layer, must also be corrected for compaction and attenuation of the spots. (D. C. Phillips, 1954 and 1956).

2.3 Peak Intensity Measurements

The determination of peak intensities by the direct photometry of X-ray photographic film has been described by Wallwork and Standley (1954). The photometer used was a HILGER non-recording photoelectric micro-photometer. A standard calibration film of the crystal being investigated was prepared first. The processed calibration film was then placed on the photometer and the exploring light beam and photocell aperture adjusted so that the illuminated area of the film projected onto the photocell was slightly larger than that of the largest reflection on the calibration film. The galvanometer sensitivity was adjusted to give full-scale deflection for clear film base and the deflections corresponding to the transmission of each of the spots were recorded.

The optical density, D , of the reflection is defined:

$$D = \log_{10} (t_0/t)$$

where t_0 = transparency of clear base

and t = transparency of the reflection.

Transparency is the ratio of the light intensity in the incident beam (I_0) to that in the transmitted beam, (I), i.e. $T = \frac{I_0}{I}$. For X-ray film, D is proportional to exposure at constant intensity, provided D is not too high. A density-exposure curve is then prepared. The curve is used to convert densities into relative intensities, since relative exposures at constant intensity and relative intensities at constant exposure are

essentially the same over wide limits. When determining the intensities of actual X-ray reflections the film is placed on the photometer and the light beam and photocell aperture adjusted as before. This is only necessary when the sizes of the largest reflection on the two films are dissimilar but the procedure ensures that the instrument is operated at maximum sensitivity. The galvanometer sensitivity control is adjusted to give full scale deflection for clear film base (P.units). Two measurements are then made for each reflection. One for the reflection and its immediate background (α units) and another for an adjacent piece of film at the same $\sin \theta$ as the reflection, (β units). The values $\log (P/\alpha)$ and $\log (P/\beta)$ are then calculated. These values are used to obtain the corresponding intensities from the calibration curve and the intensity of the reflection is obtained by subtraction.

Errors in intensity exceeding 10% are reported to arise only when the variations in area of the reflections on the same film is 2 to 1 or greater; and when the transparency, ($T = \frac{I_0}{L}$), is 60% or greater. The linearity of ILFORD G and B X-ray film is reported to extend up to about 55% transparency.

The authors consider their method of determining intensities superior to that of the visual method and that it fulfils the accuracy requirements for all normal purposes.

Furthermore, S. C. Wallwork has used this technique, since its inception, in his investigation of the crystal structure of molecular compounds exhibiting polarisation bonding (Harding and Wallwork, 1955).

Critchley and Jeffrey (1965) have also used a photometric technique

(Jeffrey, 1963) in estimating a set of peak intensities with an estimated accuracy of 8%.

Buerger (1960) draws attention to a fact of some importance in connection with peak intensities; namely, that they are not necessarily proportional to integrated intensities for the following reasons.

- (1) The same integrated intensity for small θ regions has different peak heights and consequently peak intensities

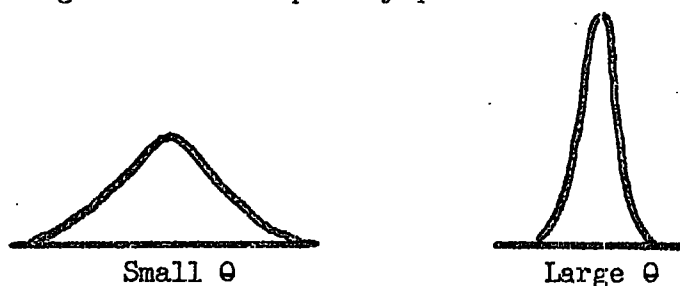


Fig. 2.1 INTENSITY PROFILES (1)

Also at large values of θ the K_{α} reflection is resolved into α_1 and α_2 doublet.

- (2) Due to crystal imperfections, the same area of peak shown in Fig. 2.1 may well have different peak heights for different reflections of the same θ value.
- (3) Peak intensities from upper layer Weissenberg rets. have to be corrected for obliquity and attenuation effects.

These reasons indicate an integrated intensity to be a more reliable measurement than a peak intensity for the same reflection.

2.4 Integrated Intensity Methods

The definition of an integrated intensity depends on the recording technique. R. D. Burbank has discussed the meaning and measurement of integrated intensities (1964) and absolute integrated intensities (1965)

in relation to the automatic diffractometer. The integration of reflections on photographic film may be performed either by a Weissenberg camera, fitted with an integrating device, (Wiebenga, 1947, Wiebenga and Smits, 1950) or by a photometer (Robertson and Dawton, 1941, Fasham and Wooster, 1958).

The photometric determination of integrated intensities is more difficult than the determination of peak intensities because of the uneven distribution of the silver grains across a reflection. Each region of the reflection thus has a different intensity and the integrated intensity consists of a sum of the individual intensities. The chief difficulty in measuring integrated intensities photometrically is that the light transmission of the blackened photographic film, which is usually measured, is not a linear function of the intensity of the reflection. Several techniques have been devised to circumvent this difficulty. An account of these is given in the next sections.

2.4.1 The Astbury α -ray method

Astbury (1927, 1929) and Robinson (1930) devised a photographic method for obtaining integrated intensities. By means of the bichromated gelatin process a reproduction of the photograph is made on a thin membrane whose thickness decreases with increasing opacity of the original. The integration over the spot is achieved by measuring, on an electrometer, the transmission of α particles, from a polonium source, through the membrane. The disadvantage of the method lies in the photographic processing of the X-ray photograph; for this reason the method does not seem to have come into general use.

2.4.2 Light Scattering Method

Brentano (1945) devised a photometric method based on light scattering. In this method use is made of the fact that, for small densities, light scattering by silver particles is proportional to the number of particles. However, the method does not seem to have been applied to a structure analysis.

2.4.3 Density Wedge Methods

Densities may be determined by balancing a reflection on an X-ray photograph with a known density on a density wedge. The point of balance is determined by a double-beam technique. One beam passing through the photograph and the other through the wedge, the position of the wedge is adjusted until the two densities are equal. Robinson's (1933) photometer integrates each photographically recorded intensity point by point. He recommends dividing the spot into 100 to 300 periodically spaced samples. Each point is balanced by moving a calibrated wedge, the balancing conditions being determined electrically. A reciprocating rod measures the motion of the wedge for all the sampling points and records their sums on a counter. The photometer is mechanically complex, tedious and slow to use. Table 2.1 contains relative intensities obtained from this instrument and from an ionisation spectrometer; the planes refer to the anthracene structure (Robertson, 1933)

15
Table 2.1

Intensities (anthracene) - arbitrary scale

<u>hkl</u>	<u>Ionisation Spectrometer</u>	<u>Robinsons Photometer</u>
200	1000	982
201	652	645
202	253	258
001	711	667
002	192	194
003	52	59
004	81	72
005	32	31

These results indicate the accuracy of the photometer to be similar to that of the ionisation spectrometer.

2.4.4 Positive Film Photometry, Dawton (1938)

This method has been used by M. J. Buerger since 1941 and requires meticulous practical techniques for it to be successful. The entire photographic procedure needs to be carefully controlled, including making the original exposure, developing the negative, exposing the second exposure through the negative and developing the positive print. The resultant positive print of the original single crystal X-ray negative consists of a collection of transparent spots on a dense black background. The total transmission of each spot is determined photometrically (Wood and Williams, 1948) and is directly proportional to the total energy reaching the spot in the original X-ray exposure. Thus transmission is directly related to integrated intensity.

2.4.5 Plateau Method

Integrated intensities may be recorded on a Weissenberg camera by means of a device designed by Wiebenga (1947). This device causes the cylindrical camera to undergo a slight rotation about the axis of the cylinder and a small additional translation parallel to the axis of the cylinder. This mechanism causes an X-ray reflection to expand over a small area of the film. The expansion smears out the reflection from a peak to a plateau, Fig. 2.2. The plateau region is in the centre of the expanded area and since within this region the film has received contributions from all parts of the expanded spot, the height of the plateau is a measure of the integrated intensity.

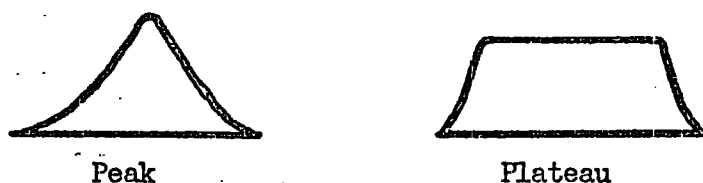


Fig. 2.2 INTENSITY PROFILES (2)

A disadvantage of this technique is that it requires about twice the normal exposure times with a proportionate increase in background density. The general scheme has been applied to the Precession camera (Nordman et al., 1955).

J. W. Jeffrey (1963) describes a photometer designed to measure the optical density of integrated Weissenberg reflections obtained by Wiebenga's technique. The photometer has been developed as part of a programme for achieving the highest possible accuracy in the photographic measurement of X-ray diffraction intensities. It has no optical or

electronic components, contains a fixed working shelf, and utilises a stabilised power supply. The light source lamp is a 24v 60w headlamp bulb; the photometer box contains a selenium photocell and the readings are made by means of a galvanometer and a cylindrical scale; in order to avoid corrections to straight scales because of non-linearity. A circular light beam of 0.5 mm radius shines on the integrated reflection whose central area should be at least 0.6 mm square. The photocell is swung into position and a reading taken, ϕR . The reflection is replaced by a portion of uniform background and another reading taken ϕB . The optical density, D , of the reflection is calculated; $D = \log \frac{\phi B}{\phi R}$. Temperature variations require the time between readings to be kept to a minimum, although, measurable drift is observed only after 5 to 10 minutes. To check this drift the scale is zeroed periodically and adjusted to give a reasonable deflection at the lower end of the scale, for a piece of film, whose background density is of the order of 0.2 D . Errors arising from the measurement of optical density by the photometer are reported as less than 1% over the density range 0.1 to 1.4 D . The percentage error increases at lower densities but is still below 5% at 0.01 D . Below 0.01 D the spots are barely visible.

2.4.6 Photometric Scanning Techniques

A different technique for determining integrated intensities was introduced by Robertson and Dawton (1941). The instrument is based on the principle of a rapid scan of the X-ray reflection, similar to the scanning used in a television tube. The reflection is scanned by a small spot of light which is passed into a photocell and amplified. By

means of a non linear circuit the amplified pulse is related directly to density and hence to the integrated intensity of the reflection. The electrical system has a quick response, of the order of 1/1000 sec. and the whole reflection can be scanned in about 0.1 sec. Its accuracy for weak reflections is reported equal to Dawton's positive film photometer and for moderate intensities is as good as Robinson's photometer, described in section 2.4.3, these being the alternative photometers available at that time. The novel features of the instrument are of course the scanning technique and the non-linear circuit. These principles have been incorporated in a more recent instrument, namely, the Joyce-Loebl integrating microdensitometer. This instrument incorporates an electronic scanning device, a non-linear electrical circuit and an integrating device which sums log L's. The instrument is described and discussed in greater detail in Chapter Three.

Fasham and Wooster (1958) introduced the concept of measuring integrated intensities by moving the X-ray film under a scanning light beam at a uniform velocity, in such a way, that all parts of the reflection are sampled. The path of the scanning beam may take several forms e.g. it may zig-zag, spiral, or move along equidistant parallel lines. However, Wooster (1964) comments that diffraction spots are usually too small for accurate photometric measurement.

He estimates that for a circular spot having a Gaussian density distribution and a peak density of 2.0 D the overall diameter must be at least 2 mm in order to reduce the error in intensity due to spot size to less than 1%. Reflections can be increased in size by using an X-ray

beam which converges on the crystal, this can be achieved by a collimator with a larger aperture at the X-ray tube end than at the crystal end, such a device lessens the exposure time.

The Wooster Automatic Recording Integrating Microdensitometer Mark III (1964) is manufactured by Crystal Structures Ltd., Cambridge. The instrument is of the double beam type and measures the light transmitted through a film by comparison with that transmitted through a neutral wedge. Optical density is automatically recorded on a built-in strip chart recorder. Utilising a single lamp and photocell the intensity record is independent of variations in output of the lamp and in sensitivity of the photocell. It is a null balance instrument and incorporates an integrating device which provides integrated intensities of lines, spots and areas. A magnified image of the parts of the film being examined may be projected onto a screen. Optical densities from 0 - 4 D may be determined with a reproducibility of $\pm 1\%$, but no data with regard to the accuracy of the instrument or of its having been used for a structure analysis is available.

2.5 Accurate Intensity Measurements by Photographic Methods

Errors arising from the photographic recording of X-ray intensities have been investigated by J. W. Jeffrey and K. M. Rose (1964). They point out that the maximum accuracy is limited by the errors inherent in the recording method. These errors have been investigated by means of photometer measurements on simulated integrated Weissenberg photographs and actual diffraction photographs. The results indicate that with careful development e.g. using filtered solutions in a thermostatic

10

bath with paddle agitation every fifteen seconds, and correct photometric techniques (Jeffrey, 1963), the standard deviation in intensity is about 0.006 D or 0.5% of the greatest intensity measured. The maximum intensity measurable is limited by the linearity of the X-ray film and Jeffrey and Rose (1964) report the linearity of ILFORD INDUSTRIAL G to extend to about 1.2 D. Even after allowing for additional factors, such as, photometer errors and the lack of uniform absorption on the top film of a pack, the total error is still less than 1% of the maximum intensity of about 1.2 D. In many cases errors inherent in the photographic record are small compared with other errors. Those due to absorption effects are frequently more significant than errors from any other single source, (Jeffrey and Rose, 1964). In the determination of the crystal structure of dimeric trimethyl 4:6 dioxonyl platinum ($\text{Pt O}_2\text{C}_{12}\text{H}_{24}$)₂ by Swallow and Truter (1960) they estimated that the variation in intensity produced by absorption in the crystal used was at least 10%. At least two thirds of the R value of 7.6% is thought to be due to absorption errors.

The main requirements for reducing recording errors in X-ray intensity measurements towards a value of 1 to 2% total error in relative $|F^2|$ values have been discussed by Jeffrey and Whittaker (1965). They recommend careful attention to detail and the elimination or reduction of systematic errors. They also discuss various experimental requirements for accurate X-ray intensity measurements by photographic means. Some of the more important of these are:

- (a) Wherever possible, crystals should be shaped into spheres or

cylinders in order to simplify or remove the necessity to correct for absorption.

- (b) The smallest collimator giving the required uniform area should be used.
- (c) Unit cell parameters must be known to 0.1% in order to calculate accurate equinclination angle settings.
- (d) Density is a function of both exposure and development time. Van Horn (1951) has shown how film linearity may be extended by the use of long developments. Consequently developing conditions should be standardised and rigidly followed.
- (e) The visual or photometric technique of intensity measurement should be designed to give the greatest accuracy.
- (f) Finally, all the intensities should be correlated and put on a common scale.

2.6 Automatic Diffractometry

2.6.1 Introduction

A diffractometer is an instrument which uses a quantum counter for measuring both the intensities and the positions of diffracted X-rays.

Automatic single crystal diffractometers provide a record of the corrected structure factors of every reflection allowed by a single crystal. Many are computer controlled and operate on the basis of programmed information. This information enables the diffractometer to set up crystal and counter angles particular to each reflection. The intensities of the ensuing diffracted X-rays are then measured by means of a quantum counter.

Geiger-Müller tubes have been used for some time for the measurement of X-ray intensities (Cochran, 1950). In recent years however they have tended to be replaced with the more sensitive 'proportional counter' and 'scintillation counter'.

Some aspects of these counters are reviewed in the following sections.

2.6.2 Geiger-Müller Counters

Geiger-Müller counters are more sensitive to X-rays than photographic film. About 10^4 to 10^5 quanta are needed to produce minimum blackening on an X-ray photograph.

Geiger counters can detect this level of energy with an accuracy of better than 0.1% and can detect over 50% of the quanta entering the tube (Sullivan, 1940). This type of counter consists of a cylindrical metal cathode within which is located a coaxial metal wire anode immersed in a noble gas atmosphere. In order to reduce the discharge, produced when an X-ray quantum is absorbed, a small amount of methylene bromide, may be used as a 'quenching agent'.

The efficiency of this type of tube has been increased by making the windows of mica and sealing this directly to the cathode cylinder. Such a construction reduces the 'dead space', which is that part of the tube in which X-rays are absorbed but not detected. The function of any counting device is to 'count' the number of X-ray quanta entering the tube at any given time. A single 'count' in a Geiger counter is a measure of the discharge produced when a quantum of X-radiation enters the tube. This is measured by recording the voltage pulse developed by

the discharge. For any Geiger counter there is a minimum threshold voltage required for a discharge. A plot of counting rate against applied voltage (Fig. 2.3) shows a plateau at which counting is independent of applied voltage. For good stability it is recommended (Lonsdale, 1948) that a Geiger counter be operated at about 100 volts above its threshold voltage.

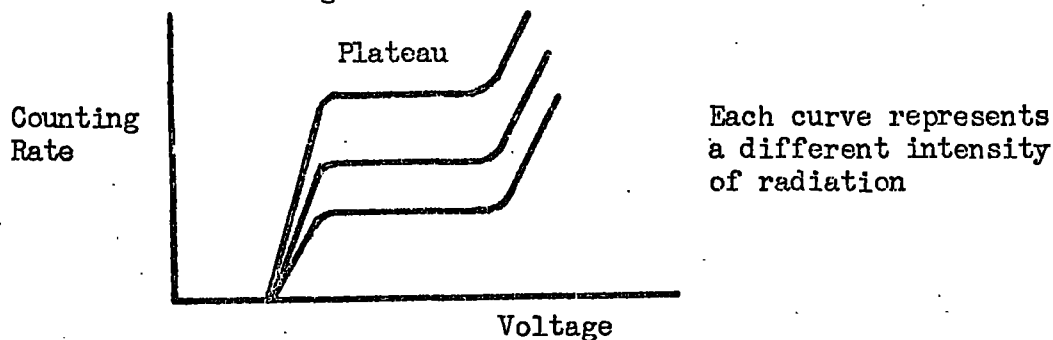


Fig. 2.3 Geiger Counter: Counting Rate Versus Applied Voltage

The proportionality between intensity and counting rate represents the linearity of response of the counter. For individual quanta to be separately recorded their arrivals must be separated by a certain time interval. This is the 'dead time' of the counter. For Geiger counters it is of the order of $50 - 300 \mu$ sec (Lonsdale et al., 1962). At low intensities, with quanta arriving at widely spaced intervals each one under ideal conditions is counted. Intensity is thus proportional to counting rate. With increasing intensity of the diffracted beam a state is eventually reached when the proportionality between intensity and counting rate breaks down. The actual point at which this occurs depends to some extent on the efficiency of the recording apparatus used. The recording apparatus consists essentially of a circuit which accepts the amplified output from the Geiger-Müller tube and provides the mean value

of the rate of arrival of counter pulses. The linearity between amplified output and counting rate limits the use of this type of recorder to low intensities (Lonsdale, 1948). Various estimates have been made for the limiting counting rate which incorporates the proportionality between counting rate and intensity and also lies within the linear range of the recorder.

Lonsdale reported 100 - 150 counts per second (1948), Bleeksma et al. (1948) reported 600 counts per sec. More recently however Lonsdale et al. (1962) reported that counting rates of 2,000 - 5,000 counts/Sec may be obtained. The life of the average counter is of the order of 10^9 counts.

2.6.3 Proportional and Scintillation Counters

Proportional counters have two fundamental advantages over Geiger counters. These are:

- (1) The construction is such that the proportionality between X-ray quantum energy and pulse amplitude is achieved. Consequently by means of a pulse-height analyser, discrimination against unwanted radiation is possible.
- (2) The dead time of about 0.2μ sec means the response is linear to very high counting rates i.e. 10^7 counts/sec. The essential features of the construction which result in these advantages include the following:
 - (a) Dead space is eliminated by having the mica window in the side of the counter. The mica window is gold plated on the reverse side in order to produce a

uniform electrical field. This construction ensures proportionality between the X-ray quantum energy and the pulse amplitude.

- (b) A slightly larger window is placed opposite the first to prevent the unabsorbed beam from striking the metal walls and causing fluorescence and unwanted pulses (Kohler and Parrish, 1955).
- (c) The gas absorption path is shorter than in the Geiger tube and a gas with a higher absorption must be used to maintain quantum counting efficiency. Xenon at 30 cm or Krypton at 50 cm Hg pressure are commonly used.
- (d) The operating voltage is below the Geiger threshold so that discharge is limited to the region where the absorption of X-ray quanta occurs. The resultant pulse amplitudes are consequently lower and have to be amplified about 10^3 times. The circuitry of a proportional counter is consequently more extensive than that of a Geiger counter where amplification of the pulse amplitude is not usually necessary.

Scintillation counters have two essential parts:

- (1) a fluorescent crystal, and
- (2) a photomultiplier tube.

The fluorescent crystal may be a single crystal cleaved plate of optically clear NaI activated with about 1% thallium in solid solution

(Hofstadter, 1949). The crystal face on the X-ray beam side must be undeformed since absorption occurs in a thin surface layer. The crystal is hygroscopic and must be hermetically sealed. Kohler and Parrish (1956) have used an aluminium holder with a beryllium window 0.13 mm thick to admit the incident X-rays and a glass back to transmit the visible light scintillations. Light reflectivity is increased by placing a bright aluminium foil 1μ thick between the beryllium window and the crystal. The internal section of the holder is shaped and highly polished. A mounting fluid, of about the same refractive index as the glass, attaches the holder to the end of the photomultiplier tube. The entire system is in a light tight cylinder. The colour of fluorescent light (violet) from the crystal matches the spectral sensitivity of the photomultiplier tube. The fluorescent decay time is only about 0.2μ sec., and the dead time is consequently about the same as that of the proportional counter. The Quantum Counting Efficiency (E), discussed on page 27, is dependent on the X-ray absorption in the crystal. For a NaI Tl crystal, about 0.55 mm thick, it is about 100% for all commonly used X-ray crystallographic wavelengths. This is better than can be achieved with either organic scintillators or polycrystalline scintillation screens (Marshall, Coltman and Hunter, 1947).

An important property of this type of counter and one which is most useful in connection with single crystal diffractometry is that its radial sensitivity is practically constant. This represents an advantage over the type of counter which absorbs X-rays through a mica window. In the latter case careful alignment is necessary in order to absorb the

radiation, whereas, the scintillation counter is able to detect X-rays through a wide angular field. By the careful choice of crystal size it is possible for a scintillation counter to intercept and detect the entire X-ray beam. The photomultiplier used usually has a low noise and an amplifier gain of 210 - 1,000 is required.

The life of the counter is practically unlimited unless water vapour penetrates the crystal holder seal.

A comprehensive account of the factors influencing the linearity of counters has been made by Lonsdale et al. (1962).

Some of these factors are included in the following comparative account of the linearities of currently available counters.

It has already been pointed out in section 2.5.2 that Geiger counters are linear up to about 5,000 c/sec. Various attempts have been made to improve on this figure by reducing the dead time of the counter tube below the range 50 - 300 μ sec (Eastabrook and Hughes, 1953, Parrat, Hempstead and Jossem, 1952). In no case however has the dead time been reduced to the level of the scintillation and proportional counters.

The multiple foil technique (Lonsdale, 1948) provides a means of correcting for non-linearity at high counting rates. The observed intensity Nobs can be corrected for non-linearity by means of:

$$N \text{ true} = N \text{ obs} (1 - \tau \text{ eff} N \text{ obs})$$

where $\tau \text{ eff}$ is the dead time of the entire system.

A monochromator is used to reflect the characteristic X-rays into the counter and a number of metal foils (e.g. aluminium), each of the

20

same absorption, are added to the beam, one at a time. This technique increases the effective dead time of the entire system and decreases the counting rate to an extent dependent on the number of metal foils used. The measured rate (N_{obs}) may then be related to the true rate (N_{true}) by means of the above relationship. A plot of N_{obs} on a log scale against the number of foils on a linear scale shows the limiting linearity and provides a means of determining τ_{eff} . The correction is easier to apply to peak intensities than to integrated intensities because of the continuous variation of the counting rate in the latter case (du Pre, 1953).

It is essential that only monochromatic radiation is measured in this technique and this may be achieved by either (a) pulse height discriminator or (b) operating the X-ray tube at a low voltage in order to avoid generating radiation of wavelength $\lambda/2$. Linearity may also be extended by measuring the average current of the counter instead of counting individual pulses.

The linearity of proportional and scintillation counters depends on the dead time of both the counter and the recording unit. The dead time for proportional and scintillation counters is of the order of 0.2μ sec. Scaling circuits usually have a dead time of about 1.0μ sec. The dead time of the pulse-height analyser depends on the distribution of the amplitudes of the pulses it receives. The linearity of the analyser depends on the dead time and the rate of arrival of the pulses at the analyser. Analysers are available which have linear rates in excess of 15,000 c/sec.

21

Scintillation counters have been shown to be linear up to about 10^7 c/sec (Nelson and Ellickson, 1955).

In the selection of a suitable counter for X-ray analysis an important factor is the 'Quantum Counting Efficiency' (E). This is defined:

$$E = f_T \cdot f_A$$

where f_T is the fraction of incident radiation transmitted through the window and dead space of the counter,

f_A depends on the length and pressure of the gas path in the Geiger and proportional counter or on the thickness of the scintillation crystal (Taylor and Parrish, 1955, 1956).

Variations in E are caused by several factors, including the following:

- (a) lack of radial sensitivity of the counter
- (b) failure of the counter to detect certain peaks i.e. escape peaks
- (c) lower absorption by the gas or crystal at low values of λ causes E to diminish
- (d) increased window absorption at high values of λ causes E to diminish
- (e) abrupt changes in E at absorption edges in the NaI.Tl crystal and proportional counters may be encountered.

Variations in the quantum counting efficiency of the counter may cause changes in the background level of X-ray patterns, especially near strong reflections.

The scintillation counter has the highest and most uniform E for all crystallographic wavelengths i.e. about seven times greater than either the Xenon proportional or the Argon geiger counters for Mo K_α radiation. This allows a decrease in recording time by a factor of 7 for the same statistical accuracy, or an improvement in accuracy by $\sqrt{7}$ using the same recording time.

The applications of each detector cannot be sharply defined but there are areas within which certain types of detector can be used advantageously.

The Geiger counter has the advantage of simple electronic circuitry coupled with high, uniform sensitivity and long life. Its disadvantages are low counting rate, low quantum counting efficiency, especially at low wavelengths and no pulse height discrimination.

Proportional counters are capable of high counting rates. The Xenon filled proportional counter has a low quantum-recording efficiency for the shorter wavelengths. Consequently pulse height discrimination is not necessary in this case, although it does decrease the recorded background. The Krypton proportional counter has a higher sensitivity to short wavelengths and a lower sensitivity to long wavelengths than the Xenon counter. A consequence of this is the lower peak to background ratio (P/B) when used with wavelengths greater than 1 Å.

The scintillation counter is characterised by high counting rates, low resolution time and high radial sensitivity. Its uniform quantum counting efficiency over all normally encountered X-ray wavelengths makes it complementary to the Krypton proportional counter. The Krypton

proportional counter may be used for low wavelengths, i.e. less than 1 \AA (Parrish and Taylor, 1955), and the scintillation counter may be used for longer wavelengths i.e. greater than 1 \AA .

2.7 Comparison of Currently Available Methods

Estimates of the errors inherent in the visual method of determining intensities vary from about $\pm 10\%$ to about $\pm 20\%$ of the actual intensity values. In spite of this the visual method is still the most widely used means of obtaining intensities from photographic film. Why then have photometric techniques failed to replace the visual method? Obviously they have not satisfied the basic requirements of greater accuracy, reproducibility and speed. The two photometric techniques currently available viz. the Wiebenga-Jeffrey method and the Joyce-Loebl integrating microdensitometer at least offer the advantage of an integrated intensity determination as opposed to a peak density determination. Jeffrey's claims for his method are impressive, he quotes a recording range extending from about 0.01 D to about 1.2 D with a standard deviation of 0.006 D (see section 2.4). In a published structure analysis, (Jeffrey and Rose, 1968) in which he used his technique, the photometer used was the Joyce-Loebl-Walker recording microdensitometer, (Jeffrey and Whittaker, 1965). This photometer provides an accurate and highly reproducible specular density determination but because of its lateral movement across the film must be rather awkward to use for Weissenberg films. This fact, coupled with the calculations involved for each reflection, must increase the time for each intensity determination considerably. It is conceivable that the technique is much slower

than the visual method. The satisfactory nature of the intensity method is indicated by an R value of 0.042 for cobalt mercury thiocyanate, $\text{Co}(\text{NCS})_4\text{Hg}$, and by the fact that the carbon and nitrogen atoms were clearly distinguished in the presence of a considerable proportion of heavy atoms, (Jeffrey and Rose, 1968).

The Joyce-Loebl integrating microdensitometer, coupled with a standard digital converter, is capable of determining about 40 reflections per hour when in the hands of an experienced operator. The recording range of the instrument is much lower than that claimed by Jeffrey, viz. from about 0.1 D to about 0.7 D as opposed to 0.01 D to about 1.2 D. However it is pointed out in greater detail, in chapter four, that the limitation is due to the film and not to the instrument. This instrument must certainly be faster than Jeffrey's generally. After a series of tests (Raper, 1966) and a satisfactory structure analysis (see chapter five), there seems to be no reason why it should not prove satisfactory as a general means of obtaining integrated intensities from photographic film. The future of any photographic method however must be seriously in doubt with the advent of the automatic diffractometer.

Comparisons of the two techniques have been made by Lonsdale et al. (1962) and Abrahams (1963).

The photographic method provides a comprehensive and permanent intensity record over large and specified regions of reciprocal space. By means of Weissenberg and precession techniques many reflections may be recorded at any one time. Furthermore, it is relatively quicker to

check an intensity determination from an X-ray film than to redetermine an intensity by means of the automatic diffractometer.

It is possible however to proceed much more rapidly to a set of structure factors, $|F_o|$, by means of an automatic diffractometer. Abrahams (1963) has compared the relative times involved in the determination of about 1,000 independent reflections. In this case the time required to obtain the photographs involves at least a month. The intensity determinations correlation and reduction of the data to a single set of 1,000 $|F_o|$'s involves several weeks of full time activity. There is also the possibility that even after all this effort the intensities could be in error to the extent of about 20% greater or less than the true value. By using an automatic diffractometer the total time spend in measuring 1,000 intensities may be reduced to less than a week. The actual time depends on the precision and overall accuracy required. With a precision of better than 1% and an accuracy of 5 to 10% it is possible to measure about 200 intensities in twenty-four hours. In addition to speed, the automatic diffractometer exceeds the photographic method in accuracy. Determination of intensities by automatic diffractometers to within 4% of the probable true values are reported by Abrahams et al., (1965 and 1967). The same worker reports that even the best photometric techniques are liable to have errors of the order of $\pm 10\%$ of the actual intensity (Abrahams, 1963).

In the near future visual and photometric methods of determining intensities will continue to be used. However, as the technology of automatic diffractometry advances and the availability of the technique

widens it is likely to become the general method for obtaining the intensity record.

CHAPTER THREE

THE JOYCE-LOEBL INTEGRATING MICRODENSITOMETER

THE JOYCE-LOEBL INTEGRATING MICRODENSITOMETER3.1 Function

The instrument provides a measurement of the total light absorption of a scanned plane area. The indication of absorption is given on a meter and is called the integrated density value (I.D.V.) The I.D.V's. may also be recorded on an analogue digital converter which can be connected to the I.D.V. meter.

Intensities of reflections on both Weissenberg and precession films may be recorded.

The I.D.V. of a reflection and its immediate background is recorded, then the I.D.V. of an adjacent blank area. The difference between these two readings is the I.D.V. of the reflection and can be compared with similarly derived I.D.V's. for other reflections. Thus relative I.D.V's. on an arbitrary scale are obtained. A circuit diagram of the instrument is shown in Appendix I.

3.2 Principle of Operation

The area of the scan, or raster, on the surface of the scanning tube, is governed by two controls which adjust the length of sweep along the X and Y directions. The raster is reduced in size and brought to a focus on the surface of the X-ray film and the area to be investigated is placed within the raster. Light is transmitted through this area to a photomultiplier. The photomultiplier is connected to an amplifier by means of a non-linear circuit. The amplified output is proportional to the logarithm of the instantaneous value of the light absorption or alternatively to density (D) and hence to the blackening of the film.

When recording I.D.V's, a single vertical sweep, viewed on the monitor tube, is used. The time for one sweep depends on the size of the scanned area and varies from 0.3 to 2.0 seconds. During a vertical sweep period the density signal is passed to the integrator where the sum of the instantaneous density values is derived and recorded on the I.D.V. meter. The circuitry is so arranged that integration occurs only during the vertical sweep period. A picture of the scanned area is reproduced on the face of the monitor tube which is synchronous with that on the face of the scanning tube. By passing a portion of the density signal to the monitor tube via an antilogarithmic circuit the visual appearance of the scanned object is reproduced within the monitor tube raster.

3.3. General Description

The instrument consists of two parts, consisting of a scanning unit and a monitor unit.

The scanning unit is a light tight box and has a door on the front for access to the specimen focussing and scanning tube focussing control.

The scanning tube is a cathode ray tube whose electron beam performs the scanning operation. This scanning technique is known as the 'flying spot method'. The scanning tube is mounted on the top of the box and can be rotated through 180° to enable alignment of the raster with elongated reflections. A microscope assembly focusses the raster on to an X-ray film which is contained within two glass plates on a moveable table. The table is positioned in a horizontal plane by two servo motors (X and Y) which are push button operated on the monitor section. A

microswitch, operated by opening the door, cuts off the power supply to the photomultiplier circuit and prevents saturation effects and possible damage to this component from ambient lighting. The photomultiplier is located in the base of the scanning unit.

The monitor unit contains most of the operating controls i.e. the monitor tube, peak density and I.D.V. meters; a facsimile table which carries a duplicate film and moves synchronously with the scanning unit table mentioned previously.

In addition there are also the following controls:

Brilliance and Contrast

These refer to the monitor tube and function in a similar manner to their counterparts in a domestic television set. The brilliance control sets the general background level of the raster and is kept constant, the contrast control is used to modify the appearance of the picture on the monitor tube.

Set Zero

This controls the brilliance of the raster on the scanning tube. The peak density meter moves in sympathy with the set zero control the brightest raster occurring at zero density. Usually the set zero is adjusted against the normal background of developed, fixed, but unexposed, X-ray film, so as to produce a peak density value in the region 0 to 0.05 D. The set zero is never used to counteract varying background density on the same piece of film as this leads to erroneous results. The control can be used to counteract a gradual drift away from the original background density setting.

X and Y Shift Controls

These shift the raster horizontally and vertically, with respect to the monitor tube, on both scanning and monitor tubes. The setting is usually that which reproduces the raster in the central portion of the monitor tube.

X and Y Sweep Controls

The horizontal and vertical size of the raster is set by these controls. There are six positions for each control, at position 6X and 6Y the raster has its maximum size being about 1.5 cm square on the face of the scanning tube and about 3 mm square on the surface of the X-ray film.

Scanning areas of about 3 mm square are most unusual for X-ray reflections. The average area is about 0.5 mm square and this is achieved with values of X and Y equal to three.

The X sweep control operates by changing the velocity of the 'flying spot' and the sensitivity of the integral meter is inversely proportional to the value of X.

The Y sweep control varies the time for each vertical sweep, the number of lines in the scan also changes, but not the spacing between the lines and the sensitivity remains unaltered.

X and Y Position Indicators

These counters give an indication of both table positions relative to the lower left hand corner as starting or zero position. It is possible to allocate X and Y table coordinates to each reflection.

Table Lock Switch

The facsimile table motors are isolated by moving this switch into

the 'UP' position. It is then possible to move the specimen table independently to align the specimen and facsimile films.

Table Drive Push Buttons

These move both tables and also the image on the monitor tube in the same direction along X and Y coordinates. They are used in conjunction with a blue spot which is projected from below onto the facsimile film in order to locate a reflection. The blue spot indicates the approximate centre of the raster field on the surface of the specimen film.

Read View 1 View 2 Switch

These three switch positions select the instrument function:

View 1 provides a constantly scanned image of the reflection on the monitor tube.

View 2 operates as for View 1 but the extinction selector switch is brought into operation.

Read used to take a measurement of background or of a reflection. The integrator is brought into circuit and the vertical sweep operates on a single shot basis. Repetition is achieved by means of the reset and integrate buttons. The monitor image of the spot is not visible during this operation.

Extinction Switch

This operates when View 2 is selected. The switch is calibrated from 0.5 to 1.5 D in steps of 0.2 D, and estimates all portions of the image of greater density than the value selected. The eliminated portions appear as bright areas within the black spot. Hence it is possible to assess whether a small or a large area of the reflection has density

greater than the value selected. If the set zero is set at a value other than 0 D against a blank i.e. background portion of the film e.g. 0.1 D then the extinction value will be the difference between the two readings e.g. $0.7 - 0.1 = 0.6$ D. This device is used to sort out reflections which are beyond the known linear range of the film. The extinction circuit does not provide a precise value of peak density and values should not be relied on to closer than ± 0.1 D (Paul, 1967).

Integrate and Reset Buttons

These are used in conjunction with the read switch. Momentary pressure of the integrate button initiates a single vertical sweep and the integrated output from the measuring circuit during this sweep is stored as a charge in the integrator. The integrator is returned to rest by pressing the reset button.

Analogue Digital Voltmeter

This device converts analogue current into an arbitrary digital value and is directly connected to the I.D.V. meter.

Calibration of the digital voltmeter is achieved by setting it to zero when the I.D.V. meter is zero and to 1,000 with the I.D.V. meter at its maximum value of 2,500. The analogue digital voltmeter is a much more sensitive recording device than the I.D.V. meter. It provides a continuous scale from 0 - 1,000 in divisions of one. Each division on the I.D.V. meter has a value dependent in the scale used e.g. 10 on the 500 scale, 20 on the 1,000 scale and 50 on the 2,500 scale.

3.4 Operating Procedure

The instrument is usually allowed to warm up for at least fifteen

minutes before making measurements so as to allow the components to reach a stable temperature. Reasonable precautions are needed to ensure stable temperature conditions e.g. avoidance of direct sunlight. The screen of the scanning tube is easily burned and the sweep is never left stationary during the warming up period; the scanning tube brilliance is also reduced during warming up periods or if the instrument is to be unused for any length of time. The film to be measured is placed in the specimen frame and the copy in the facsimile.

The films are then aligned in their frames until the reflections are coincident. Then the clamping screws are tightened and the frames placed in their respective tables. Weissenberg films have to be cut across the middle in order to accommodate them in the frame but precession photographs fit into the frame without cutting.

The tables are aligned by positioning a suitable reflection on the facsimile frame above the blue locating spot. This table is then locked by the appropriate switch. The corresponding reflection on the specimen frame is then aligned by means of a light beam and an inclined mirror, located under the specimen table, which projects an image of the chosen reflection onto the surface of the scanning tube. The reflection is then centred in the raster on the scanning tube surface. Both tables are now aligned, and after releasing the locking switch, respond synchronously to the table drive control.

Reflections are measure whose peak densities occur within the linear range of the film. Peak density is recorded by switching to VIEW 2 and advancing the extinction switch from 1.5 towards 0.5 until a brightening

of the central part of the reflection is observed. The switch position at which this is observed indicates the peak density of the reflection relative to its background. Background peak density is set by means of the set zero and READ control to a definite value e.g. 0, 0.05 or 0.1 D. So with a background density of 0 the peak density is as recorded, otherwise, subtraction is necessary. The limiting density which marks the end of the linear range is 0.7 D. All reflections which have peak densities in excess of this value are not recorded.

Having verified that a reflection is within the linear range of the film the VIEW 2 control is switched to READ, the reset button is pressed, to eliminate any residual charge in the integrator, and the integrator button pressed. This procedure is repeated until a constant reading is observed on the I.D.V. meter. The value is then recorded, together with the appropriate hkl, on a paper roll attached to the analogue digital recorder. The record is achieved by punching hkl manually on the keyboard and pressing the READ button on the recorder to obtain the I.D.V. automatically. I.D.V.'s. of both reflection and background are recorded and the final I.D.V. punched out manually by means of the keyboard.

3.5 Instrument Evaluation

The accurate measurement of integrated intensities by the Joyce-Loebl integrating microdensitometer is subject to the following basic limitations:

- (a) instrument linearity and sensitivity
- (b) the linearity of the X-ray film used for the intensity record

3.5.1 Instrument Linearity

This is most readily demonstrated by means of an optical glass wedge. The results of a typical calibration are shown in table 3.1 and graph 3.1. They show the linearity of the instrument to extend up to about 1.5 D with a deviation of less than 1%.

3.5.2 Instrument Sensitivity

The sensitivity of the instrument is governed by the X sweep control. This operates by changing the velocity of the 'flying spot' while keeping the sweep time constant. Thus with increasing raster width, i.e. increasing X value, the velocity of the spot increases and the scanning is less efficient than at lower X values. Sensitivity is therefore inversely proportional to the X value.

In order to check the variation in sensitivity with X value an intensity scale was prepared. The scale was prepared by using a 0.3 mm collimator and passing nickel filtered copper radiation through nickel foil into a Weissenberg camera loaded with ILFORD INDUSTRIAL G X-ray film. Sixteen spots were obtained by varying the exposure times from two to a hundred seconds. Within the linear range of the film i.e. at low exposure levels, the spots were circular and about 0.3 mm diameter and at high exposure levels they were elliptical and about 1.0 x 0.6 mms. The visual intensities ranged from being just visible to the very intense. The I.D.V's. of the spots were then determined over a range of X values from 2 to 5 inclusive and at Y values 2 and 3. These were chosen as being the most likely values to find general use. The peak intensities of the spots were also determined. The I.D.V's. and peak densities are

listed in table 3.2 and plotted in graphs 3.2.1 and 3.2.2.

The results show that variations in Y sweep have little significant effect on the I.D.V's. but variations in X sweep have a pronounced effect. In general, the lower the X value the higher the I.D.V. This confirms that the sensitivity is inversely proportional to the raster width, or, X sweep value. The manufacturers claim, in the instrument handbook, that it is possible to convert I.D.V's. from one X value to another by a simple arithmetical device, e.g. if I.D.V's. have been collected at $X = 2$, $X = 3$ and $X = 4$, to convert them all to $X = 3$ simply requires that the $X = 2$ values be multiplied by $2/3$ and the $X = 4$ values be multiplied by $4/3$. Inspection of the results in table 3.2 however shows that these simple numerical ratios frequently break down. This is largely because the I.D.V's. listed were read from the I.D.V. meter and not obtained from the more accurate digital converter. Consequently, I.D.V's. in excess of 550 for $X = 2$ and $X = 3$ were recorded on the 2,500 scale, where each division represents 50 units, and all values at $X = 4$ and $X = 5$ were obtainable only from the 2,500 scale. It is more meaningful to record that most of the scaled readings agree to within one or at most two scale divisions. The best method of scaling under such circumstances is from graphs, since they take into account minor variations in the theoretical ratios.

3.5.3 X-Ray Film Linearity

Measurement of the I.D.V's. of actual Weissenberg reflections revealed that film to film scaling constants, (Rossman, 1956), failed markedly with reflections whose peak densities exceeded 0.9 D. On the

other hand, reflections with peak densities in the region 0.5 to 0.9 D generally scaled to within the experimental limits of the method.

This behaviour, presumably, results from the breakdown, at about 0.9 D, of the Reciprocity Law:

$$\text{Spot Density} = \text{intensity} \times \text{time}$$

The intensity of the X-ray beam and exposure time enter into this relationship as equal partners. It is usual to maintain steady operating conditions so as to obtain a constant intensity of the X-ray beam. Thus the Reciprocity Law can be restated:

$$\text{Spot Density} = f(\text{exposure time})$$

A plot of spotdensity, (I.D.V.), against exposure time, will be a straight line up to an I.D.V., which marks the limiting linearity of the X-ray film. In order to assess the linearity of ILFORD INDUSTRIAL G X-ray film the data from X = 4, Y = 2 was converted to the same scale as the exposure time, after excluding all values in excess of 0.9 D, i.e. those for 60, 80 and 100 secs. The values are listed in table 3.3 and plotted in graph 3.3.

They show the departure from linearity to be about 3% at densities just over 0.7 D and about 10% at 0.9 D. The I.D.V's. used in this test were obtained from the I.D.V. meter; when the instrument had been fitted with an 'analogue digital converter' it was decided to repeat the test with a different film scale. The data is listed in table 3.4 and plotted in graph 3.4, I.D.V's. and exposure times have been placed on the same scale. The lowest peak density measurable on the integrating microdensitometer is 0.5 D. Reference to table 3.4 shows that four of the

reflections on this scale have peak densities less than 0.5 D.

Peak densities for these reflections were obtained from the Joyce-Loebl microdensitometer MK III C.S. This instrument uses density wedges together with a double beam technique and provides a specular density measurement. The density of the first seven reflections were obtained on this instrument and a scale factor obtained by relating the densities at 12, 16 and 20 with the corresponding densities obtained from the integrating microdensitometer. By this means, the density values obtained from the microdensitometer were placed on the same scale as those obtained from the integrating microdensitometer, the values are listed in column (2) of table 3.4. The departure from linearity at low density is appreciable, about 35% at 0.05 D or an I.D.V. of 13, and about 13% at 0.07 D or an I.D.V. of 26, these are of course, very weak reflections. Between 0.16 D and 0.7 D i.e. within the I.D.V. range 50 to 200, the deviation is about 1%, this is the most reliable density range. At 0.9 D the deviation increases again from 5% to about 20% for the four values listed at this density. The significance of this variation at 0.9 D is that an I.D.V. is a function of size and density, being an integrated measurement. Consequently, the larger the amount of density in the spot in excess of 0.9 D, the greater is the deviation from linearity. Jeffrey and Rose (1964) report minor departures from linearity for the same film, ILFORD G, at densities well below 1.0 D. Two comparisons of commercially available X-ray film have been sponsored by the INTERNATIONAL UNION of CRYSTALLOGRAPHY (Wiebenga and Smits, 1956, Morimoto and Uyeda, 1963). The results from both investigations,

reported and compared by Morimoto and Uyeda, indicate about an 8.0% departure from linearity at 1.0 D for ILFORD INDUSTRIAL G X-ray film.

3.5.4 Accuracy and Reproducibility

Experience indicates the reproducibility of the instrument to be high; better than 2% for the same operator in the linear range of the film. Agreement between different operators determining intensities between 0.5 and 0.7 D is usually within 2% of the I.D.V's. measured. Between 0.7 and 0.9 D the agreement varies between 2% at the lower and 5% at the higher density. On average, within the linear range of the film, agreement between operators is better than 5%.

A reasonable assessment of the accuracy of a method for determining X-ray intensities will result from a comparison of observed structure amplitudes $|F_0|$ and calculated structure factors $|F_C|$, obtained from a suitable structure analysis. The most accurate result necessitates keeping the errors arising from the physical factors associated with the data record, particularly absorption effects, down to an absolute minimum. However, some assessment of the contribution to the R factor by the method could be attempted.

A less rigorous assessment can be made from Density - Exposure curves. The accuracy here is likely to be better than that from an actual structure analysis because of the absence of physical effects and the existence of a uniform background on the X-ray film. In this instance the accuracy of the method is tied to the linear response of the X-ray film, such that the limits of accuracy are confined to the deviations from linearity of the film. This is not unreasonable, since

the limitations of the method in this instance, are not instrumental but depend on the linearity of the X-ray film. Table 3.4 and graph 3.4 provide the necessary information. At low densities the error increases from about 13% at 0.07 D to about 30% at 0.05 D. From 0.16 D to 0.7 D, I.D.V's. may be measured to a standard deviation of 0.31 or 3 scale units, about 1.1%. The minimum measurable I.D.V. for a reflection about 0.05 D is in the region of 10 scale units. At 0.9 D the error varies from about 5% to about 20% depending on the size of the spot. These results agree with similar experiments made independently by the manufacturers (Paul, 1967).

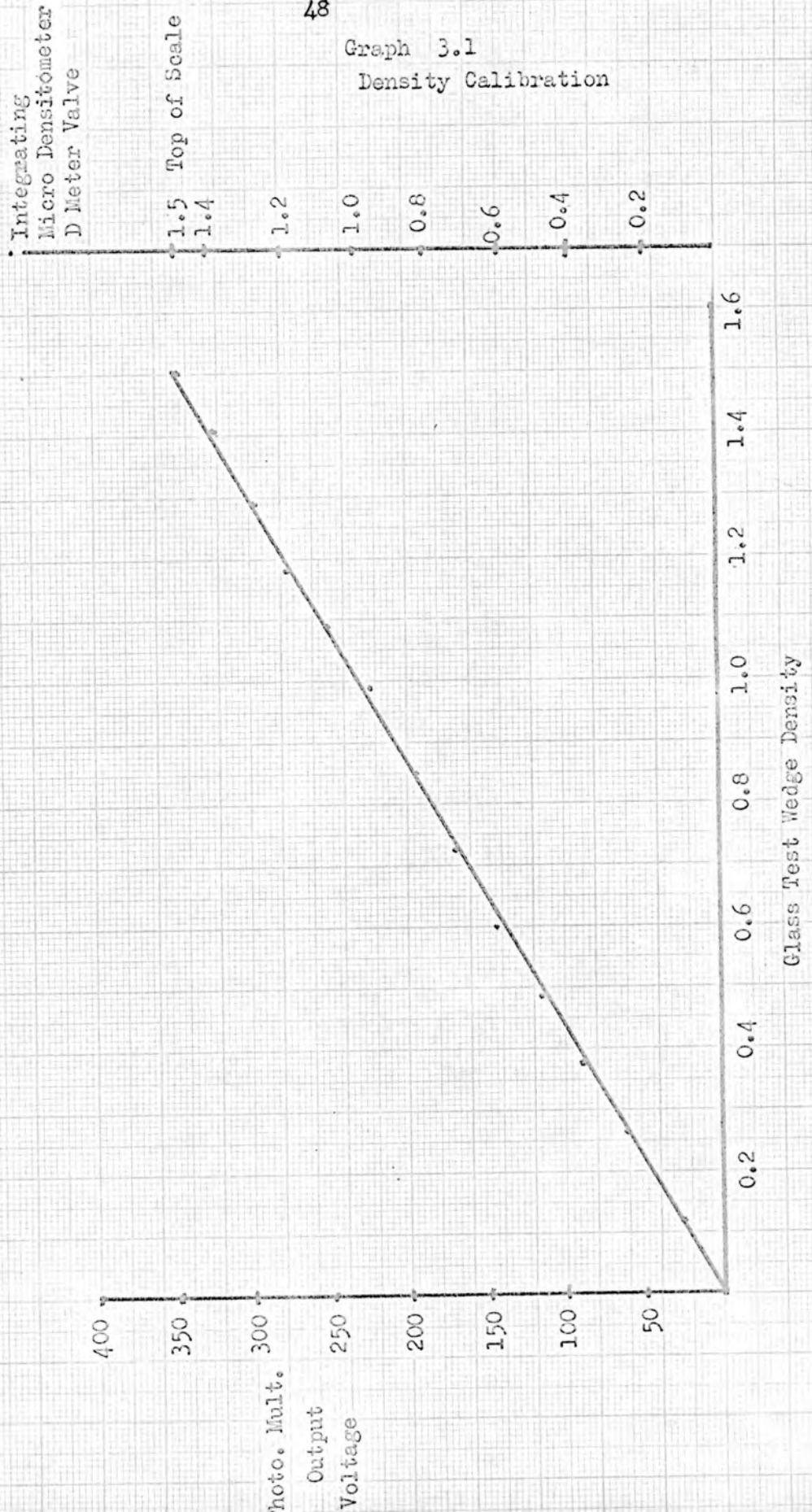
In this section, much use has been made of density values, particularly in connection with the limits of film linearity. In this context it is important to appreciate the difference between a specular and a diffuse density measurement. Density wedge methods usually record specular densities, there being little allowance for that portion of the beam which is diffused on passing through the wedge. Such densities are usually higher than those obtained from a diffuse densitometer. In the latter case the light collection is more efficient, the intensity of the emergent light beam, L , is greater than that measured by density wedge techniques, and the ratio: $D = \log_{10} (I_0/L)$, is consequently lower, for the diffuse densitometer.

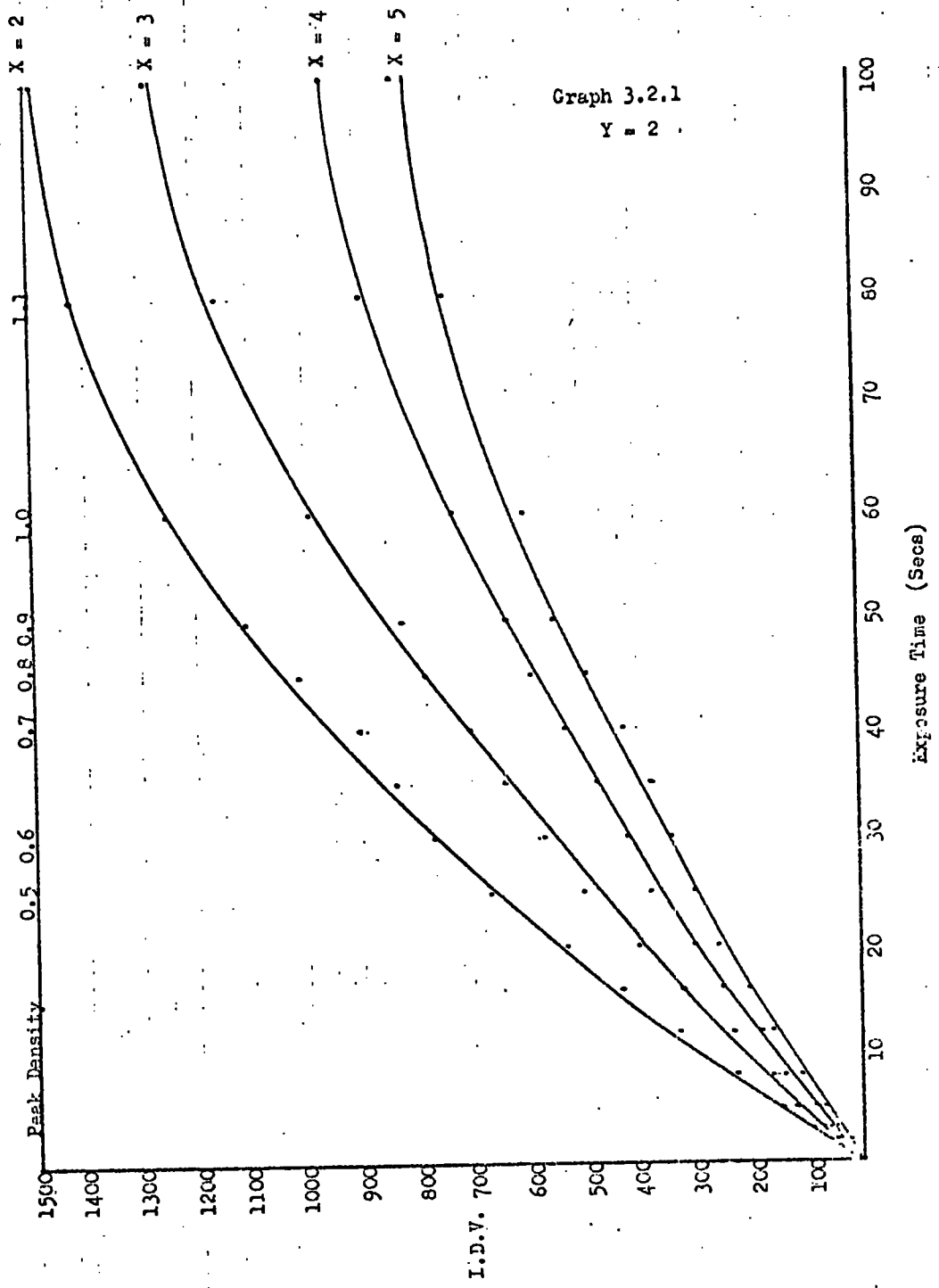
Density estimations from the Joyce-Loebl integrating microdensitometer have been compared with those, for the same piece of film, obtained from the McBETH QUANTALOG DIFFUSE DENSITOMETER (Paul, 1967). These results show the agreement between the two instruments to be

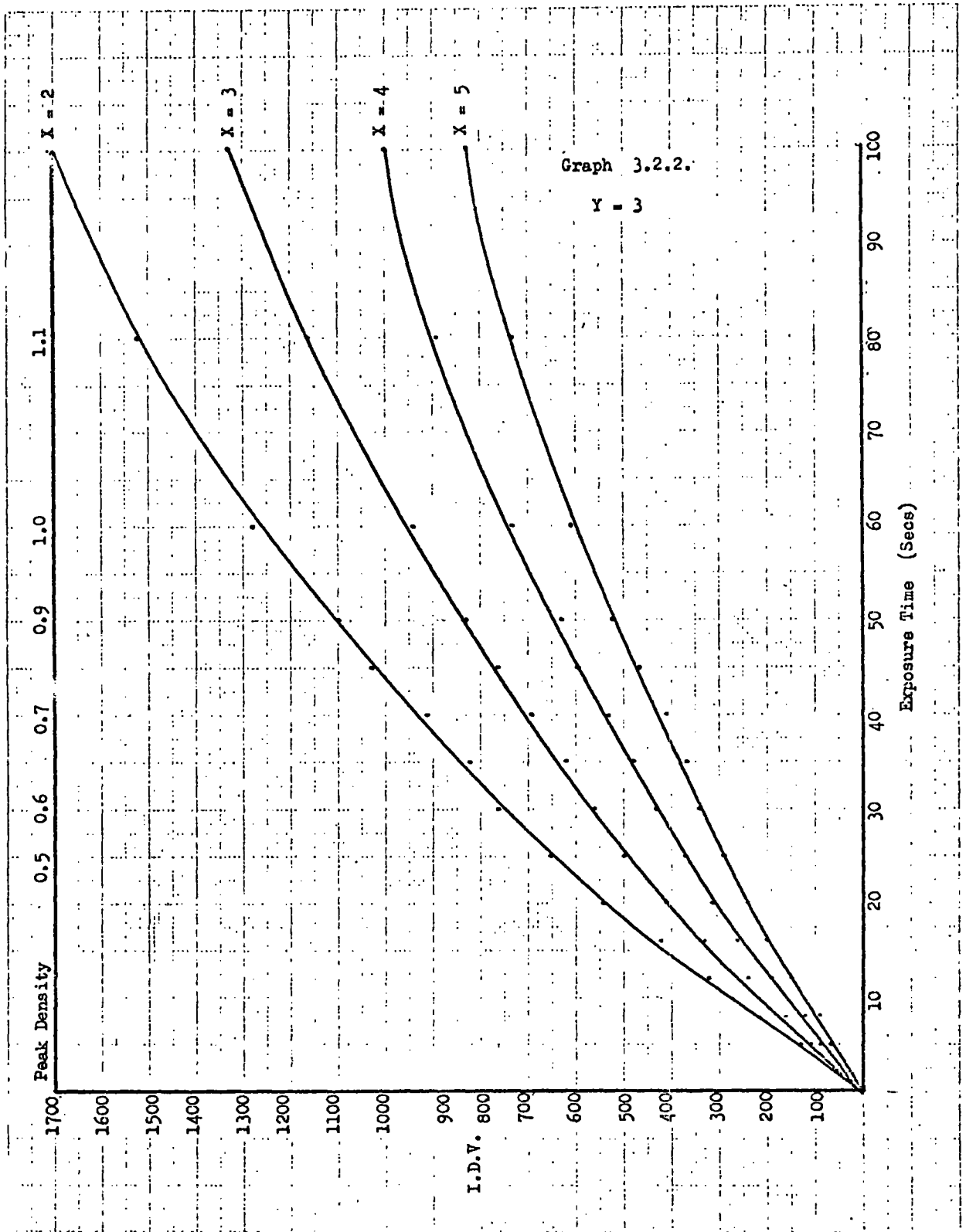
within 2% for the density range 0.1 to 1.5 D. It appears, then, that the integrating microdensitometer provides a reliable diffuse density measurement.

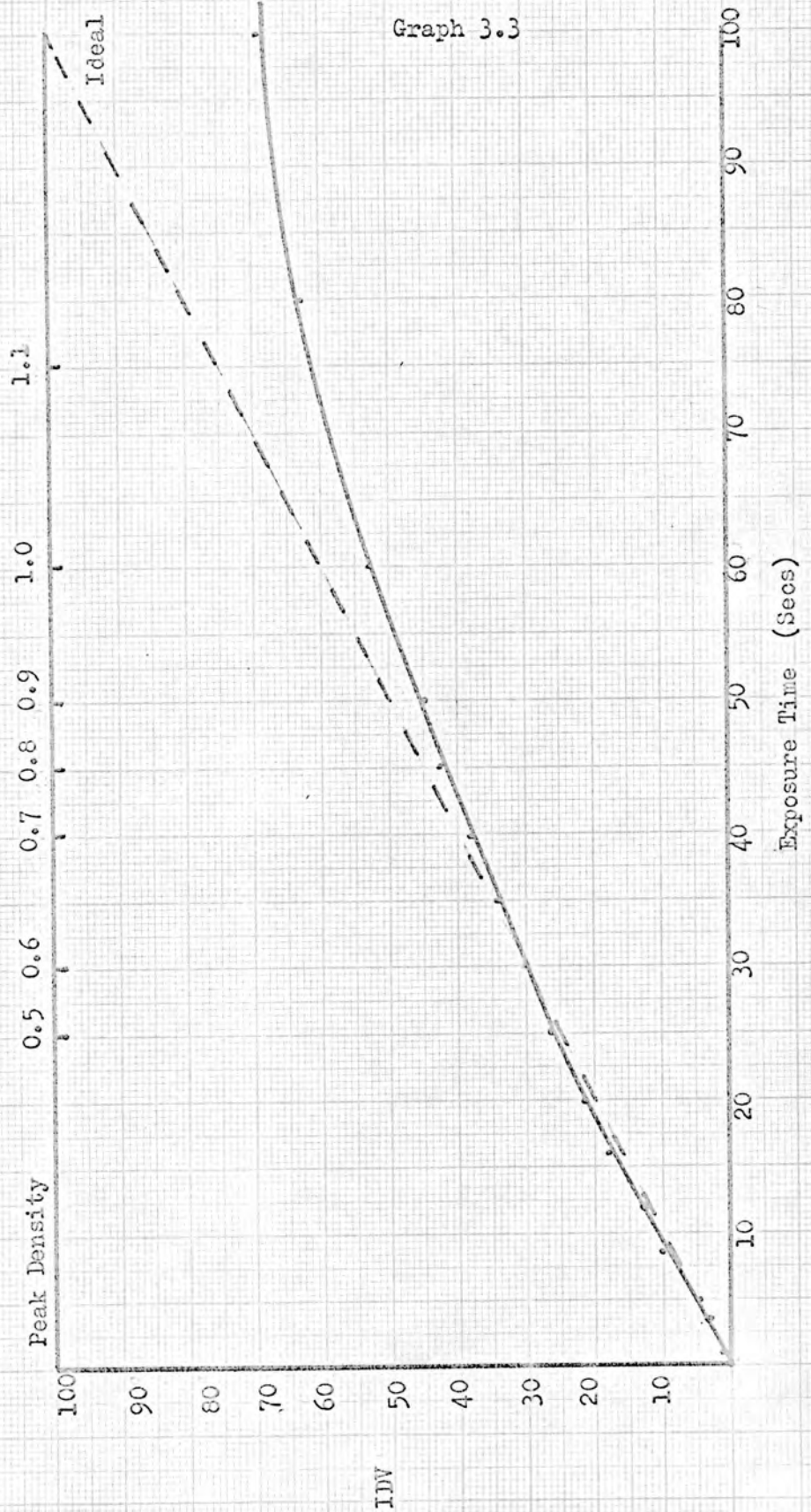
The tabulated results are contained in Appendix II.

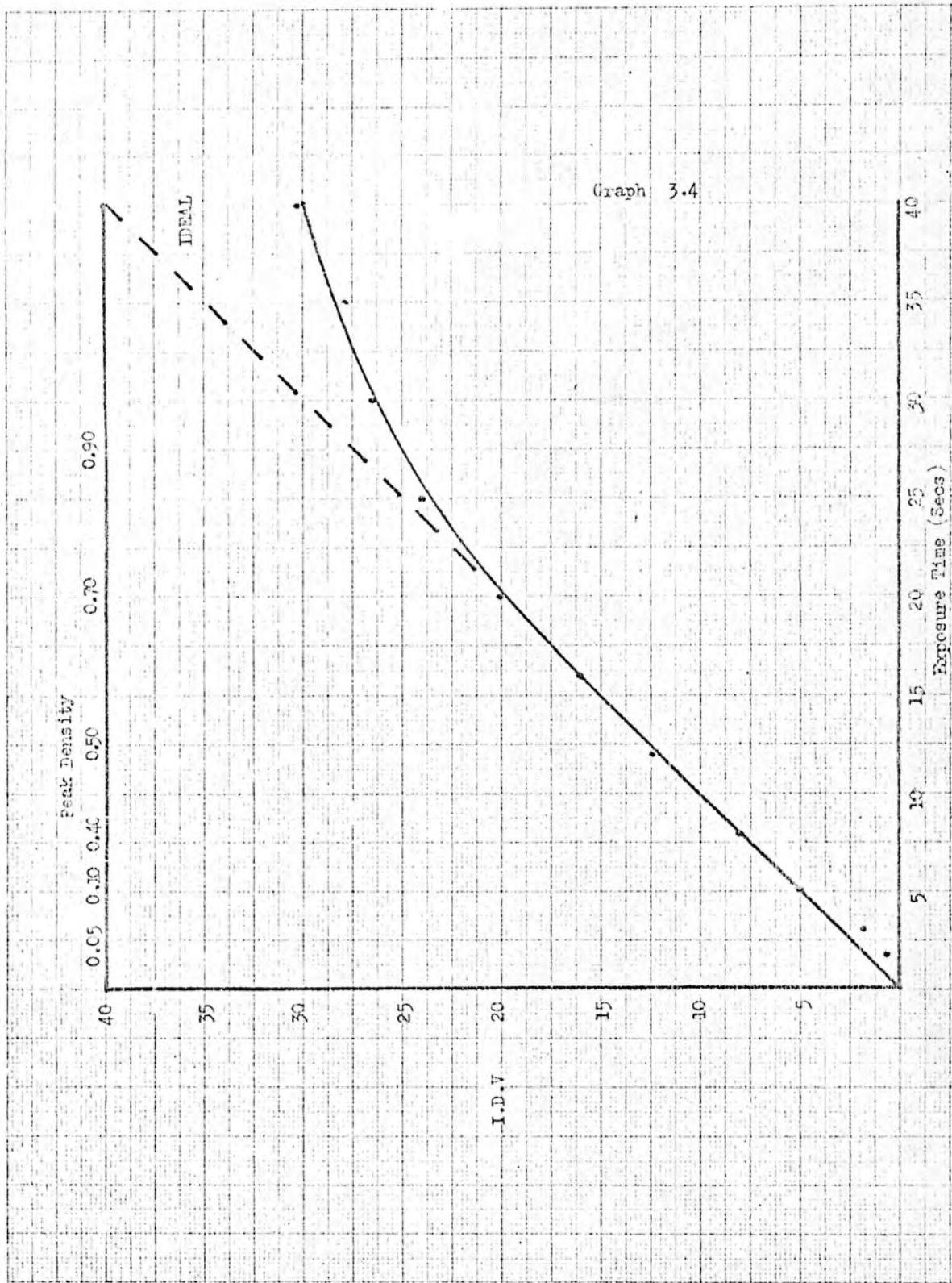
Graph 3.1
Density Calibration











CHAPTER FOUR

A COMPARISON OF DOUBLE AND SINGLE COATED

FILM RESPONSE

A COMPARISON OF DOUBLE COATED AND SINGLE COATED FILM RESPONSE4.1 Introduction

For X-ray film exposed to X-rays the relationship:

spot density ~~is~~ exposure time

is linear up to some limiting I.D.V. (see Section 3.5.2). Previous work (Raper, 1966) indicated the limiting density for Ilford Industrial G, double coated film, to lie between 0.7 and 0.9 D. The linear relationship usually holds up to 0.7 D but deviation is evident at 0.9 D. On the other hand the linear response of the Joyce-Loebl integrating microdensitometer extends up to about 1.5 D. There is obviously an appreciable discrepancy between the linearity of the instrument and that of the film. A direct consequence of this discrepancy is the limitation it places on the recording technique. In an attempt to improve the technique it was decided to investigate the suitability of single-coated film for the intensity record. Double coated film has silver halide grains on both sides of a cellulose base. This arrangement will be advantageous for low intensities presumably but there is a possibility that at higher densities the existence of silver halide grains on the reverse side of a film will facilitate rapid saturation. In connection with this problem the following points were considered:

- (a) would single coated film have a limiting density at the same I.D.V. as double coated film or would the linearity be extended?
- (b) to what extent could higher exposure levels be accommodated within the linear range of single coated film?
- (c) would there be any loss of recording efficiency at low

intensities when using single coated film?

4.2 Experimental

The film used throughout this investigation was ILFORD INDUSTRIAL G X-ray film, a double coated film. As no single coated X-ray film of the same specification was commercially available, single coated response was simulated by the inhibition of developer action on the reverse side of the double coated film. The technique used for this purpose is outlined in Appendix III.

Two sets of scales were prepared. One designed to cover the density range up to the point of complete film saturation and another to cover the lower range, from less than 0.1 to 1.0 D, in greater detail. Preliminary experiments showed that the use of a 0.5 mm collimator was adequate for the overall density range and a 0.3 mm collimator was suitable for the lower density range. Nickel filtered Cu K_α X- radiation was used and nickel foil was also used to reduce the intensity of the beam so that a barely visible reflection was obtained with a two second exposure, using the 0.3 mm collimator and double coated film. The same piece of foil was then used in each subsequent scale preparation. The two sets of scales were prepared by separately exposing duplicate films for each collimator. A Weissenberg camera was used, and the following exposure ranges employed: 2 - 380 secs for the 0.5 mm collimator and 2 - 200 secs for the 0.3 mm collimator. The individual exposures are listed in the appropriate tables in Appendix II.

One film from each set was developed for six minutes in PHENEX developer, washed for one minute in running water and then fixed for

eight minutes in ILFORD fixer. These films were then washed for one hour in running water and allowed to dry. Developer action was prevented on the reverse side of each duplicate film by using the following procedure. Each film to be processed was fixed by SELLOTAPE to a supporting sheet consisting of a slightly larger piece of unexposed, processed film; the reverse layer, being the unwanted layer, was the one in contact with the supporting sheet. Developing and fixing were carried out simultaneously with the double coated film from each set. The supporting sheet was then removed and the undeveloped emulsion hardened by immersion for ten minutes in fixing solution. Each simulated single coated film was then washed simultaneously with the conventional double coated film for an hour and dried.

All the films were processed simultaneously and agitated, manually, in their holders during processing. The resultant spots showed a variation in size. Those from the 0.5 mm collimator varied from circular and 0.5 mm diameter, within the linear range of the film, to elliptical, with dimensions about $1.5 \times 1.0 \text{ mm}^2$ at high exposure values. A similar variation was observed in the spots from the 0.3 mm collimator.

The peak and integrated intensities of the spots were measured on the Joyce-Loebl integrating microdensitometer by means of the technique outlined in chapter three. Most of the spots were measured with an X sweep value of three but the larger ones were measured with an X sweep of four, five or six. The measured I.D.V's. are recorded in the column of results labelled 'DETERMINED I.D.V.' In order to place the results on a common scale, all I.D.V's., measured with an X value other than

three, were scaled to X equal to three. The columns labelled 'I.D.V. X = 3' contain the scaled values. The lowest peak density detectable on the integrating microdensitometer is 0.5 D. In order to investigate lower peak density values, the Joyce-Loebl MK III C.S. microdensitometer was used. The peak densities of the reflections from the 0.3 mm collimator double coated film in the exposure range 2 to 20 seconds were measured on the MK III C.S. microdensitometer. These peak densities were then converted to the same peak density scale as the integrating microdensitometer. The densities are listed in column (2) of table 4.2.2.

All the tabulated results associated with this section are contained in Appendix II. Tables are included in sections 4.3 and 4.4; graphs are at the end of the chapter.

4.3 Discussion of Results

4.3.1 0.5 mm Collimator Double and Single Coated Films

Single Coated Film (See Graph 4.1.1)

The graph shows a linear portion up to about 0.7 D and then a gradual curve up to a peak density in excess of 1.1 D.

Double Coated Film (See Graph 4.1.2)

This graph appears also to have an initially linear portion followed by a gradual curve, terminating at some point in excess of 1.3 D.

The exposure at 140 secs marks the recording limit of the instrument due to the size and density of the spot obtained at this exposure level; subsequent exposures are consequently off scale.

Comparison between Double and Single Coated Films

Reference to Table 4.1.3 shows that the ratio of I.D.V's.

TABLE 4.1.3

COMPARISON OF THE I.D.V.'S. OF SINGLE AND DOUBLE COATED FILMS

0.5 mm Collimator

Exposure Time secs	Peak Density		Ratio of I.D.V.'s. (<u>Double Coated</u>) Single Coated
	Single Coated Film	Double Coated Film	
3	less than	less than	2.14
5	0.5 D	0.5 D	2.06
8		0.5	2.15
12		0.9	2.14
16	0.5		1.84
20		1.1	1.97
25	0.7		1.93
30			1.94
35			1.76
40	0.9		1.69
45			1.67
50			1.67
60		1.3	1.59
70	1.1		1.56
80			1.46
100			1.51
120			1.42
140			1.46

(double coated), is slightly in excess of 2.0 up to, and including, a peak density value of 0.9 D, for double coated film. At higher peak density values the ratio is less than 2.0. Ideally the ratio should be 2.0 up to the point at which double coated film becomes non linear.

These values show that the significant density region for double coated film extends to about 0.9 D. In order to fix accurately the point at which the linearity of double coated film breaks down, more values are needed in this lower region.

These values are those listed for the 0.3 mm collimator.

4.3.2 0.3 mm Collimator Double and Single Coated Films Single Coated Film (See Graph 4.2.1)

There is an initially linear portion extending to about 0.9 D with a gradual curve from thereon.

Double Coated Film (See Graph 4.2.2)

Again there appears to be an initially linear portion extending to about 0.9 D and then a gradual curve.

Comparison between Double and Single Coated Films

Table 4.2.3 shows the ratio of I.D.V.'s. ($\frac{\text{Double Coated Film}}{\text{Single Coated Film}}$), to be about 2.0 up to a density of 0.7 D on double coated film. Above 0.7 D the values are less than the ideal value of 2.0. The limiting density for double coated film appears to be 0.7 D.

4.3.3 The Linearity of Single Coated Film

The Reciprocity Law,

$$\text{I.D.V.} = \text{intensity} \times \text{time},$$

means that the ratio of $\frac{\text{I.D.V.}}{\text{Exposure Time}}$ should be constant for a linear

TABLE 4.2.3

COMPARISON OF THE I.D.V'S. OF SINGLE AND DOUBLE COATED FILMS

0.3 mm Collimator

Exposure Time secs	Peak Density		Ratio of I.D.V's. (<u>Double Coated</u>) (Single Coated)
	Single Coated Film	Double Coated Film	
2	less than	less than	—
3	0.5 D	0.5 D	2.00
5			2.08
8			2.11
12		0.5	2.08
16			1.98
20		0.7	2.10
25	0.5	0.9	1.87
30			1.76
35	0.7		1.57
40			1.70
45			1.75
50	0.9		1.65
55			1.61
60			1.62
65			1.60
70			1.29
75			1.41
80			1.38
85			1.37
90		1.1	1.48
100			1.49

relationship to exist.

Reference to Table 4.3.1 shows that,

- (a) for double coated film the ratio is reasonably constant up to 0.7 D
- (b) for single coated film the ratio is also reasonably constant up to 0.7 D.

Furthermore, a comparison of the I.D.V./EXPOSURE ratios for double coated and single coated film, see table 4.3.1, shows an approximately 2:1 relationship for these ratios, up to 0.7 D. This is what is expected when both films are behaving ideally.

The limiting density appears to be 0.7 D for both double and single coated film, hence the relative amount of information contained on single, as opposed to double coated film, will correspond to the ratio of the exposure values at which the limiting density is reached. For double coated film 0.7 D is reached at an exposure level of 20 secs (see table 4.3.1). In the case of single coated film the issue is complicated by the fact that three separate exposure values produce reflections with some peak density greater than 0.7 but less than 0.9 D (see table 4.3.1). These correspond to exposure values of 35, 40 and 45 secs (see table 4.3.1). Hence the possible ratios are $\frac{35}{20} = 1.75$; $\frac{40}{20} = 2.00$ or $\frac{45}{20} = 2.25$ i.e. single coated film may accommodate 1.75, 2.00 or 2.25 times the exposure values accommodated on double coated film. Ideally, one would expect a ratio of 2.00 to 1.00. A ratio in excess of 2.00 to 1.00 seems barely possible and since the reflection at 45 secs contains the largest amount of density, in the range 0.7 to 0.9, it seems likely

TABLE 4.3.1

0.3 mm Collimator

COMPARISON OF $\frac{\text{I.D.V.}}{\text{EXPOSURE}}$ RATIOS

<u>SINGLE COATED FILM</u>			<u>DOUBLE COATED FILM</u>		
<u>Exposure Time secs</u>	<u>Peak Density</u>	<u>Ratio I.D.V. Exposure</u>	<u>Exposure Time secs</u>	<u>Peak Density</u>	<u>Ratio I.D.V. Exposure</u>
3	Less than	4.3	3	Less than	8.9
5	0.5	4.8	5	0.5	10.0
8	"	4.5	8	"	10.0
12	"	4.8	12	0.5	10.8
16	"	5.1	16	0.6est	10.0
20	"	4.8	20	0.7	10.0
25	0.5	5.1	25	0.9	9.6
30	"	5.0	30	"	8.8
35	0.7	4.9	35	"	7.6
40	"	4.7	40	"	7.9
45	"	4.4	45	1.0est	7.6
50	0.9	4.4	50	"	7.2
55	"	4.4	55	"	6.9
60	"	4.3	60	"	6.5
65	"	4.0	65	"	6.1
70	"	3.8	70	"	5.2
75	"	4.0	75	"	5.1
80	"	3.7	80	"	5.0
85	"	3.6	85	"	4.9
90	"	3.5	90	1.1	5.1
100	"	3.2	100	"	4.8
110	1.0est	3.1			
120	"	2.9			
130	1.1	2.9			
140	"	2.8			
150	"	2.7			
160	"	2.5			
170	"	2.4			
180	"	2.3			
190	"	2.3			
200	"	2.3			

that the peak density here is nearer 0.9 than 0.7. The I.D.V./EXPOSURE ratio at 45 secs is 4.4 as opposed to 4.4 and 4.9 at 40 and 35 secs respectively and about 5.0 within the linear range of the film. This indicates a significant departure from linearity at 45 secs and therefore the ratio 2.25 can be discounted. Single coated film appears to be able to accommodate between 1.75 and 2.00 times the exposure level of double coated film. It would be useful to have more values in the exposure range 35 to 40 secs as this would provide a more accurate assessment of the ratio. It is feasible that the apparent departure from an ideal ratio of 2.0 to 1.0 is due to the increased sensitivity of single coated film.

Graph 4.3.1 shows that the I.D.V./EXPOSURE ratio decreases much more rapidly in the case of double coated film after the linear range has been passed. This indicates a much more rapid departure from linearity, with increasing exposure time, for double coated as opposed to single coated film. Reference to table 4.2.3 shows that the ratio of I.D.V.'s. of double to single coated film is 2 to 1 up to the limiting density of 0.7 D on double coated film. This means that within its linear range both sides of a double coated film absorb equivalently. After 0.7 D the ratio drops below 2.1. It would seem that the second photosensitive layer is less efficient than the first and this would account for the rapid departure from linearity of double coated film.

4.4 Summary

There appears to be no marked increase in the linearity of single coated film, as opposed to double coated film, both becoming non linear

at 0.7 D. For an optimum spot size this peak density is equivalent to about 200 I.D.V. units at $X = 3$. Double coated film, however, reaches the limiting density at approximately half the exposure level required for single coated film. This must be a result of the existence of the second photosensitive layer which accelerates the rate of saturation of double coated film. Single coated film is therefore able to accommodate longer exposures than double coated film. Reference to tables 4.2.1 and 4.2.2 shows that the only spot lost by using single, instead of double coated, film is that which corresponds to an exposure time of 2 seconds and an I.D.V. of 13. On double coated film this exposure corresponds to a peak density of about 0.05 D, so on single coated film this would correspond to a peak density in the region of 0.02 to 0.025 D or an I.D.V. of 6. The spot produced by an exposure time of 3 secs has a peak density of about 0.07 D on double coated film and an I.D.V. of 26. On single coated film the equivalent spot is visible and has an I.D.V. of 13, half that of the double coated film, so this spot would have a density of about 0.035 to 0.04 D. The only reflections likely to be missed at the lower end of the density scale, by replacing double with single coated film, are those with densities of about 0.05 D, or less corresponding to an I.D.V. of 13, or less, on double coated film. There appears to be a minimal loss of recording efficiency at lower density levels when double coated film is replaced by single coated film.

Single coated film is also capable of a better differentiation, between reflections occurring within the same density range, than double coated film. Reference to table 4.3.1 shows that within the peak density

TABLE 1.2.1

0.3 mm Collimator

SINGLE COATED FILM

Exposure Time secs	Y Value	X Value	Determined I.D.V.	I.D.V. X = 3	Peak Density Value
2	3	3	Undetectable	-	0.5
3	3	3	13	13	"
5	3	3	24	24	"
8	3	3	36	36	"
12	3	3	60	60	"
16	3	3	81	81	"
20	3	3	95	95	"
25	3	3	128	128	0.5
30	3	3	150	150	"
35	3	3	170	170	0.7
40	3	3	186	186	"
45	3	3	196	196	"
50	3	3	219	219	0.9
55	3	3	236	236	"
60	3	3	241	241	"
65	3	3	249	249	"
70	3	3	264	264	"
75	3	3	274	274	"
80	3	3	290	290	"
85	3	3	300	300	"
90	3	3	307	307	"
100	3	3	321	321	"
110	3	3	338	338	1.0est
120	3	3	353	353	"
130	3	3	378	378	1.1
140	3	3	389	389	"
150	3	3	406	406	"
160	3	3	393	393	"
170	3	3	402	402	"
180	3	3	417	417	"
190	3	3	438	438	"
200	3	3	451	451	"

TABLE 4.2.2

0.3 mm Collimator

DOUBLE COATED FILM

Exposure Time secs	Y Value	X Value	Determined I.D.V.	I.D.V. X = 3	Peak Density Value
2	3	3	13	13	0.5
3	3	3	26	26	"
5	3	3	50	50	"
8	3	3	76	76	"
12	3	3	125	125	0.5
16	3	3	160	160	0.6est.
20	3	3	200	200	0.7
25	3	3	240	240	0.9
30	3	3	264	264	"
35	3	3	266	266	"
40	3	3	316	316	"
45	3	3	344	344	1.0est
50	3	3	361	361	"
55	3	3	380	380	"
60	3	3	391	391	"
65	3	3	398	398	"
70	3	3	365	365	"
75	3	3	386	386	"
80	3	3	399	399	"
85	3	3	413	413	"
90	3	3	456	456	1.1
100	3	3	478	478	"

range 0.7 to 0.9 one reflection was obtained on double coated and three were obtained on single coated film. Within the density range 0.9 to 1.0 four reflections were recorded on double coated as opposed to ten on single coated film. By accommodating more reflections with the same peak density and I.D.V. range than double coated film, single coated film offers the advantages of greater recording efficiency and sensitivity. Single coated film is also able to record a wider exposure range than double coated film. Consequently reflections too dense to be measured on double coated film i.e. those in the density range 0.9 to 1.0 may be measured on single coated film. This increase in recording range represents a significant increase in the number of possible measurements per film.

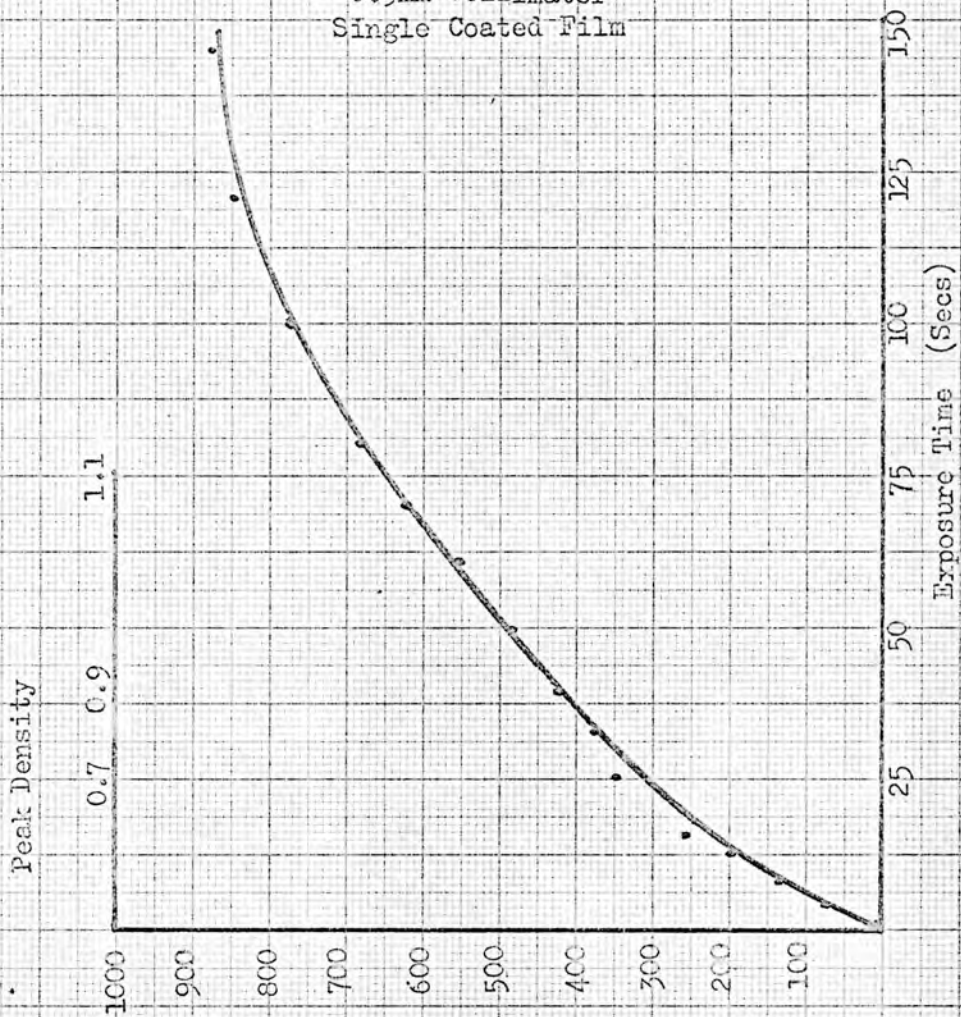
The absence of a second photosensitive layer on single coated film should cause a general lowering of background intensity.

Consequently, for the same exposure time, the ratio $\frac{\text{integrated}}{\text{background}}$ intensities should be higher in single coated than in double coated film, since the acceptable I.D.V. range is the same for both films. There should therefore be an improvement in the accuracy of the I.D.V. measurements on single coated film, particularly those regions where high background is normally encountered on double coated film e.g. low $\sin \theta$ and for weak reflections with low I.D.V.'s. Film to film scaling constants for single coated film should be lower than those for double coated film because the diffracted beam interacts with only one photosensitive layer per film.

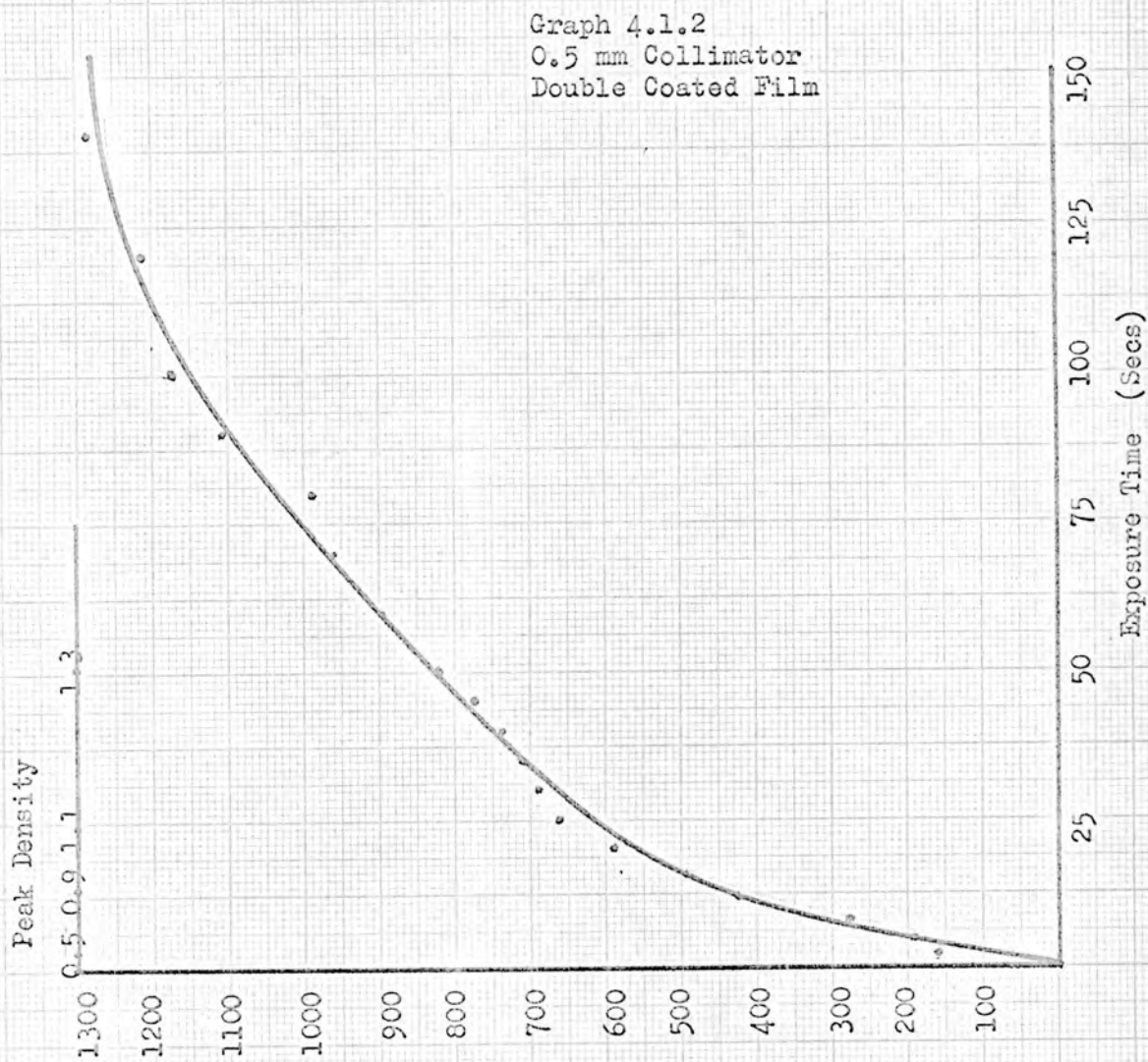
By using single, instead of double coated film in the multiple film

pack I.D.V's. of the same reflection should be closer in numerical value on successive films. Furthermore, it should be possible to record more successive values for the same reflection by replacing double coated with single coated film. In other words, six single coated films in the same pack will have a wider recording range, greater sensitivity and higher accuracy than three double coated film in the same pack. Furthermore it should be possible to achieve this without any significant increase in exposure times.

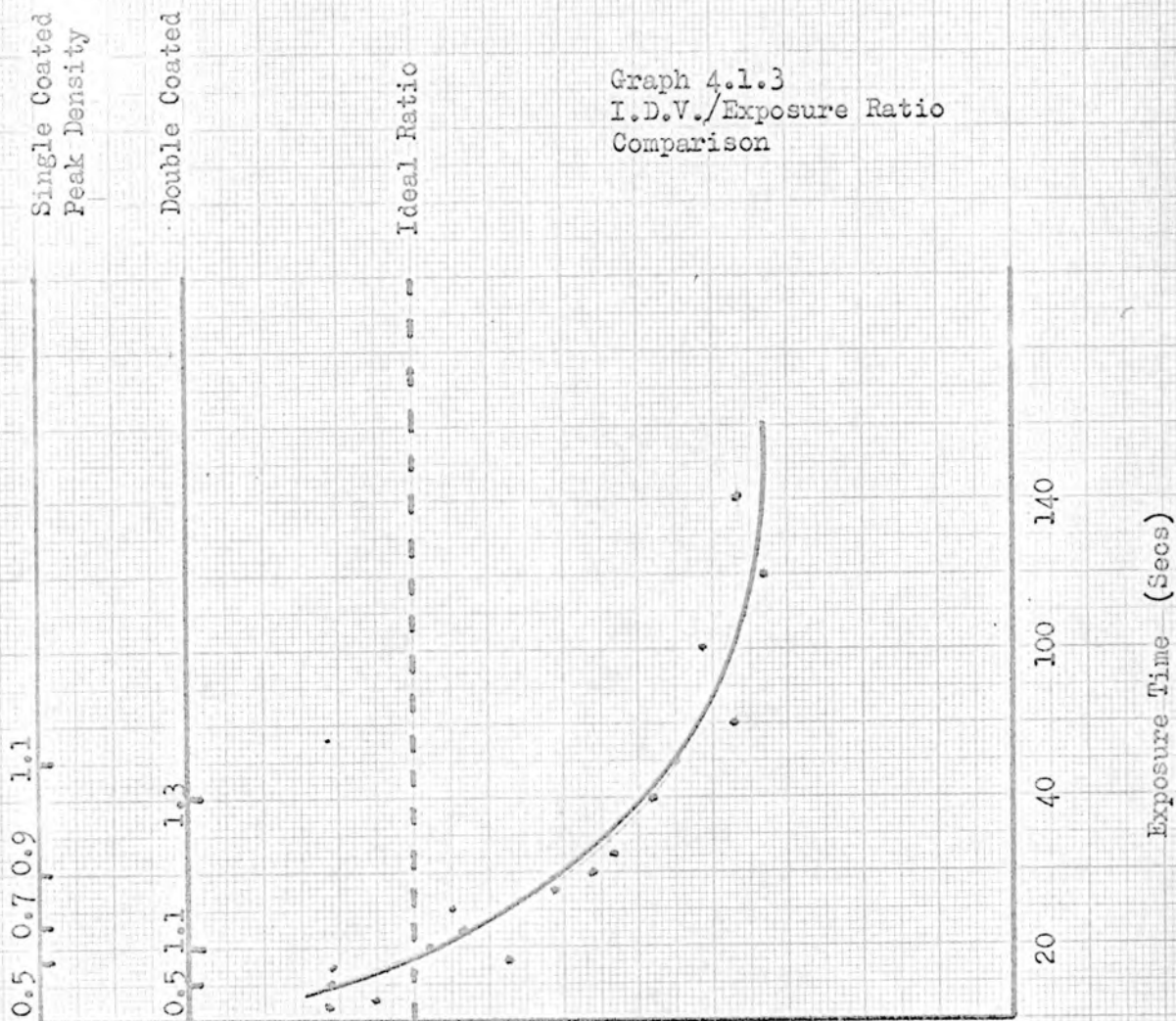
Graph 4.1.1
0.5mm Collimator
Single Coated Film



I.D.V.
X = 3



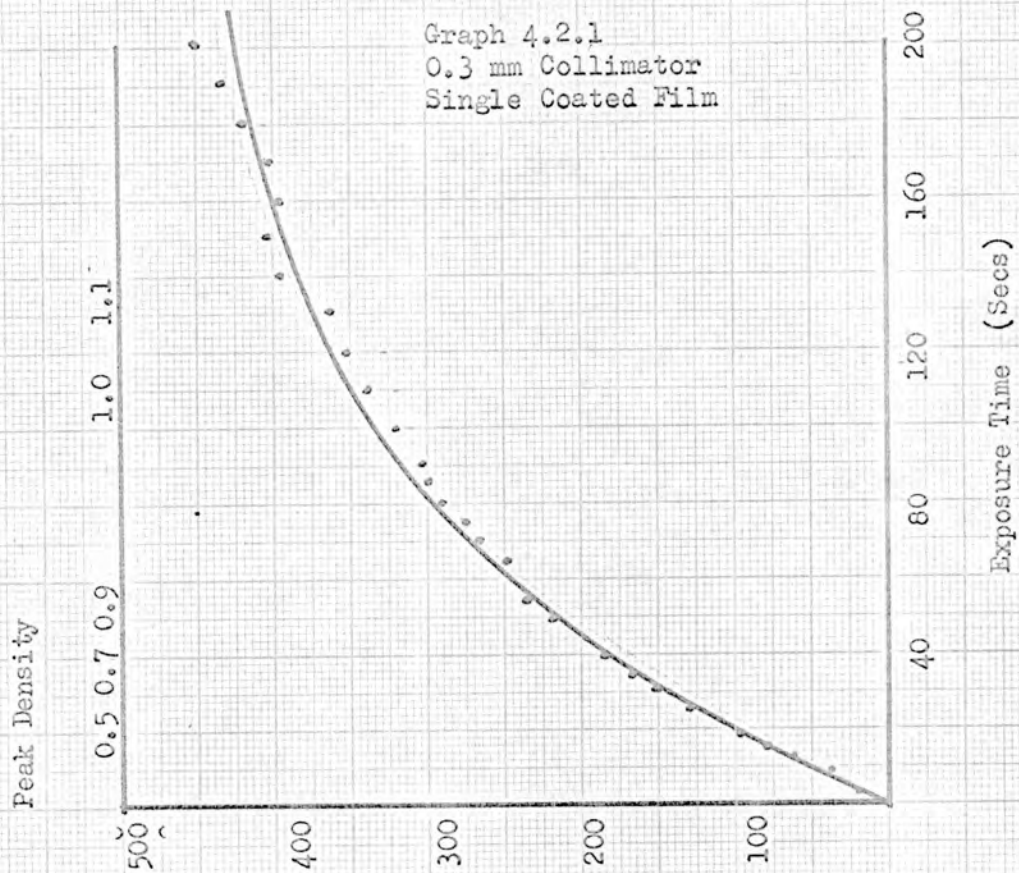
I.D.V.
X = 3



2.25
2.125
2.00
1.875
1.75
1.625
1.50
1.375
1.25

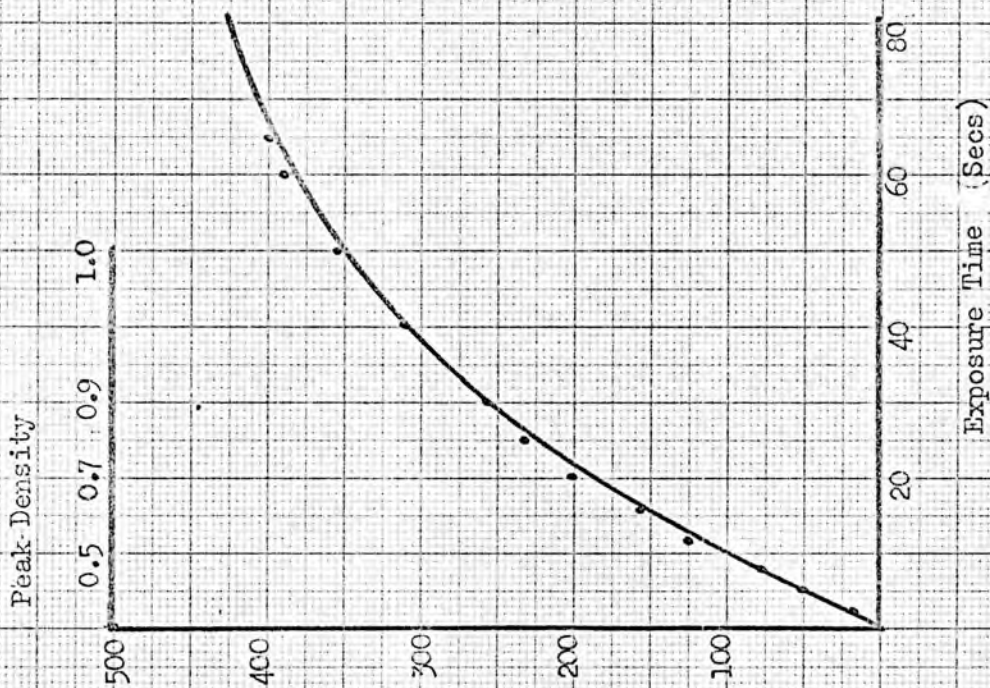
Ratio of I.D.V.

Double Coated
Single Coated

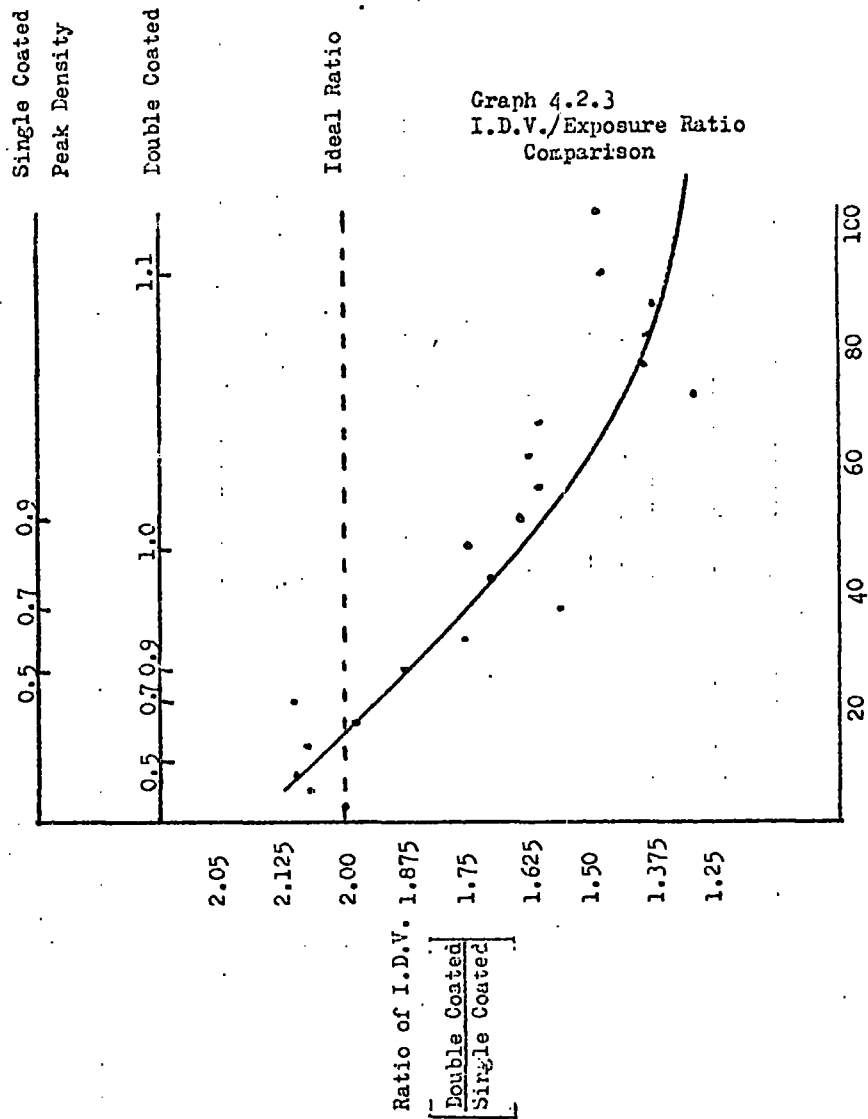


I.D.V.
X = 3

Graph 4.2.2
0.33mm Collimator
Double Coated Film

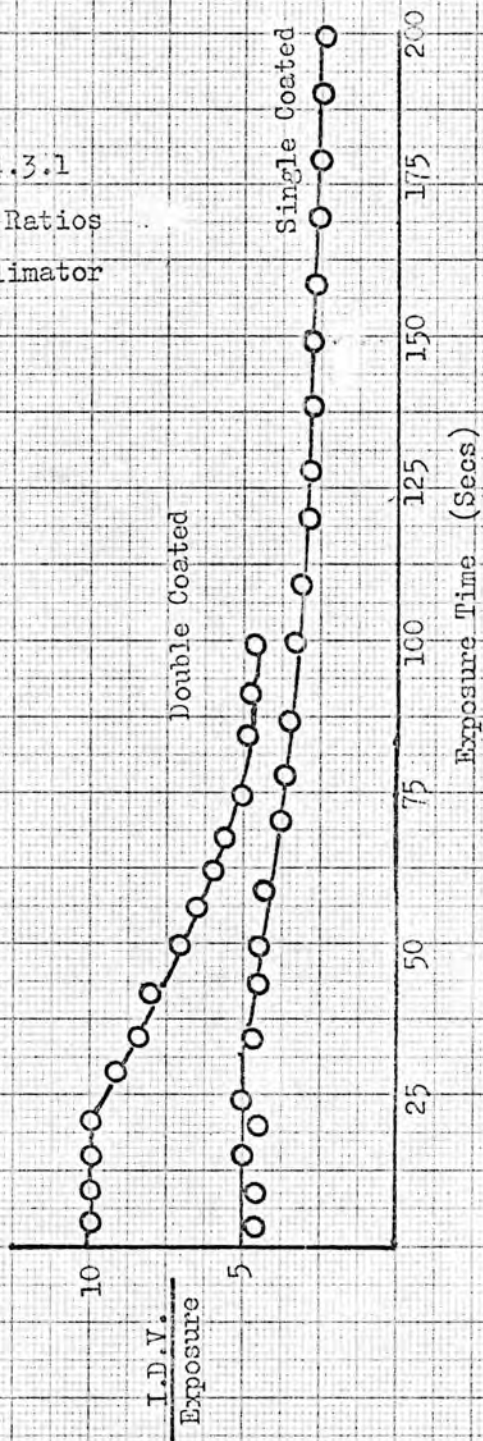


I.D.V
X = 3



Exposure Time (Secs)

Graph 4.3.1
IDV/Exposure Ratios
0.50mm Collimator



CHAPTER FIVE

THE CRYSTAL STRUCTURE OF 2-THIOAMIDOPYRIDINE



5.1 Introduction

The crystal and molecular structure of 2-thioamidopyridine, $C_6N_2H_7S$, has been studied by Downie T. G., Harrison W., and Raper E. S., in the chemical laboratories of the Rutherford College of Technology, Newcastle upon Tyne. The substance behaves as a bidentate chelating ligand to group II B metals (Sutton, 1963) and transition metals (Sutton, 1966). With group II B metals compounds of the form $[M(\text{thiopic})I_2]$ and $[M(\text{thiopic})_2][ClO_4]_2$ where $M = Zn, Cd$ or Mg , crystallise from aqueous ethanol by direct combination of the appropriate salt and the ligand, 2-thioamidopyridine, (thiopic). Among the transition metals which form complexes with 2-thioamidopyridine are rhodium (III), gold (I) and (III), ruthenium (II), chromium (III) and manganese (II). The ligand was found to coordinate in 1:1, 2:1 and 3:1 ratio with the metals e.g. $[AuCl_2(\text{thiopic})][AuCl_4]$, $[RhCl_2(\text{thiopic})_2]Cl \cdot 2H_2O$, and $[Cr(\text{thiopic})_3]Cl_3$. The formulae have been established by chemical analysis and conductivity studies.

The pyridine nitrogen atom is always involved in the bonding together with either the sulphur or nitrogen atom of the thioamido group (see fig. 5.1)

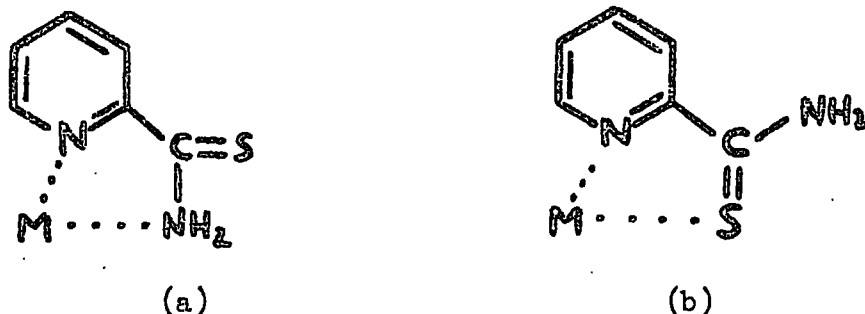


Fig. 5.1 Bonding in Metal-thiopic Chelates

Studies of absorption spectra in the visible and infra-red region of the spectrum have indicated which of the side-chain atoms is involved in specific complexes. The sulphur atom of the side-chain is involved in the rhodium (III), gold (I) and (II) complexes while the nitrogen atom of the side-chain is involved in other cases e.g. chromium (III) and manganese (II).

It was decided to attempt a structural analysis of 2-thioamidopyridine in view of its chelating ability and its possible use as a corrosion inhibitor.

5.2 Crystal Data

The substance crystallises in pale yellow needles, elongated in the 100 direction and with uniform cross-section of the order of 0.40 x 0.40 mm². The following unit cell dimensions were obtained from precession photographs using zirconium filtered, molybdenum radiation.

$$\begin{aligned} a &= 5.79 \text{ \AA} \\ b &= 7.42 \text{ \AA} & \beta &= 106^{\circ}54' \\ c &= 16.26 \text{ \AA} \end{aligned}$$

The calculated volume of the unit cell is 668.38 Å³, the calculated density is 1.37 g. cm⁻³. The observed density was determined by the flotation method and gave 1.40 g. cm⁻³. There are four molecules in the unit cell.

Inspection of precession and Weissenberg photographs gave the following conditions for reflection

$$\begin{aligned} h k l &: \text{no conditions} \\ 0 k 0 &: k = 2n \\ h 0 l &: l = 2n \end{aligned}$$

These conditions place the compound in the space group $P2_1/C, C_{2h}^5$.

5.3 Data Collection and Intensity Measurements

A Weissenberg camera and nickel filtered copper radiation were used for the data collection. One crystal was used to collect the series $h n l$ from $n = 0$ to 4 and a separate crystal was used to collect the series $n k l$ from $n = 0$ to 3. Their intensities were measured on the Joyce-Loebl integrating microdensitometer by W. Harrison, who used the technique outlined in chapter three. The bulk of the reflections were accommodated with both X and Y sweeps of 2. This places the X and Y coordinates of the reflections in the size range 0.1 to 0.2 mm. Some large reflections were measured at higher sweep values e.g. the 200 reflection was measured at $X = 5$ and $Y = 3$ and the I.D.V. scaled to the common value at $X = 2$.

An upper density limit of 0.9 was used and no reflection whose peak density was in excess of 0.9 was recorded by the instrument. Approximately 1,500 reflections were measured and only 6 of these were too dense to be measured with any accuracy, on the instrument. Intensity values were assigned to these reflections by visually comparing them with reflections of similar size and density.

The intensities were corrected for Lorentz and polarisation effects but not for spot length. The structure factors from intersecting nets were placed on the same relative scale by the method of Monahan, Schiffer and Schiffer (1967). For the common reflections an average structure factor was taken. The total independent reflections numbered 1,061.

A close agreement in the structure amplitudes $|F_{OBS}|$ was observed

among the common reflections scaled in this way e.g. the 19 pairs of values for the 22 $\bar{2}$ reflections were within 3.0% agreement of the average value for each pair. Such a close agreement seems to indicate that the intensity method is precise.

For the higher layer Weissenberg nets the upper part of the film, containing the contracted spots, was used for the intensity record in preference to the lower part containing the elongated ones. Most of the reflections from the top part of the film could be accommodated with an X sweep value of 2 whereas some of the elongated reflections in the lower part of the film required an X value of three. As the previous measurements had indicated a maximum acceptable I.D.V. of about 100, with X = 2, it was felt that there would be a significant drop in accuracy by measuring the intensities at X = 3, since the maximum measurable I.D.V. would be expected to be about 67.

On the other hand, it was felt that a maximum I.D.V. of 100 was too low for really accurate work and a maximum between 200 to 300 would be better. There are two ways of achieving this, either, by using an optimum crystal size, so as to produce reflections in the range 0.2 - 0.35 mm diameter or, by using the Wiebenga integrating mechanism to spread out the reflections. The integrating mechanism would help to reduce the peak density and increase the integrated intensity value for those reflections whose peak densities normally occur at 0.9 D and above.

5.4 Structure Analysis

The crystal structure of 2-thioamidopyridine was solved by the heavy atom method. A three-dimensional Patterson synthesis revealed a

consistent set of coordinates for the sulphur atom. These coordinates were used to calculate structure factors ($R = 0.50$) which were then used to generate a three-dimensional Fourier synthesis. This synthesis revealed, unequivocally, the positions of all the nitrogen and carbon atoms. Another structure factor calculation gave an R value of 0.265. A Fourier synthesis based on all these atoms gave improved values for the atomic coordinates. A third structure factor calculation produced an R value of 0.235.

The structure was then refined by the method of least squares using the block diagonal approximation. After four cycles of refinement with isotropic and four cycles with anisotropic temperature factors the R value reduced to 0.130. In this last cycle of refinement, the shifts in atomic coordinates were all less than the bond length e.s.d.'s. (shown in table 5.2) derived from the coordinate e.s.d.'s. obtained from the least squares totals.

Further refinement is proceeding and it is intended to calculate a difference synthesis in an attempt to locate the seven hydrogen atoms.

A list of atomic coordinates appears in table 5.1.

5.5. Description and Discussion of the Structure

A detailed description and discussion of the structure will be made when the refinement is complete. However, the results obtained so far show generally good agreement in comparison with similar systems.

Bond lengths and angles and their standard deviations are listed in tables 5.2 and 5.3, and illustrated in figs. 5.2 and 5.3.

Within the pyridine ring the C-C bond lengths are equal within

experimental error and lie in the range 1.39 Å to 1.42 Å with standard deviations varying from 0.014 Å to 0.027 Å. The C-N bond distances are given as 1.33 Å and 1.35 Å with standard deviations of 0.013 Å and 0.017 Å respectively. Microwave spectroscopy data on the free pyridine molecule (Bak, Hansen and Rastrup-Anderson, 1954) reported C-C distances of 1.391 Å and 1.398 Å and two C-N distances of 1.342 Å. In substituted pyridine compounds, e.g. pyridoxine hydrochloride (Hanic, 1966) the C-C distances vary from 1.36 Å to 1.41 Å and the C-N bond distances are reported at 1.33 Å and 1.35 Å.

These values show that the C-C and C-N bond lengths in the pyridine ring of 2-thioamidopyridine agree, to within experimental error, with similar bond lengths in the free pyridine molecule and in substituted pyridines.

The following is a comparison of the bond angles from the pyridine ring in 2-thioamidopyridine and the free pyridine molecule (Bak et al., 1954):

<u>Angle</u>	<u>2-thioamidopyridine</u>	<u>Pyridine</u>
C-C-C	117.7 to 119.0	118.1 and 118.6
C-N-C	117.7	116.7
C-C-N	122.1 and 125.2	124.0

The variations quoted for each particular type of bond angle in 2-thioamidopyridine are not significant and the values agree, to within experimental error, with the corresponding angles in the free pyridine molecule.

An interesting feature in substituted aromatic compounds is the

occurrence of a large valence angle at the point at which electron withdrawal occurs. Among the compounds exhibiting this phenomenon is pyridoxine hydrochloride (Hanic, 1966) in which the C-N-C angle is 124.5° and nitrobenzene (Trotter, 1959) in which the angle at the nitro-substituted carbon atom is 125° . It is interesting that the valence angle at the point of substitution, C(6), in 2-thioamidopyridine is 125.2° , which seems to indicate electron withdrawal by the thioamido side chain.

The C(1)-C(6) bond length is 1.53 \AA , both carbon atoms are sp^2 hybridised. The corresponding bond length in pyridoxine hydrochloride (Hanic, 1966) is 1.50 \AA . The difference between these values is not significant, although the remaining atoms in the side chain are different in the two molecules.

In the side chain the C(1)-S double bond length is 1.66 \AA and the C(1)-N(1) bond length is 1.34 \AA . The reported values for the corresponding bonds in dithio-oxamide are 1.66 \AA and 1.30 \AA respectively.

TABLE 5.1

Co-ordinates of Atoms

<u>Atom</u>	<u>x/a</u>	<u>y/b</u>	<u>z/c</u>
S	.23289	.19421	.03149
N (1)	.71135	.19267	.07829
N (2)	.77455	.49098	.16520
C (1)	.50655	.27599	.07772
C (2)	.82739	.65095	.20615
C (3)	.65122	.78256	.20204
C (4)	.40936	.74727	.15323
C (5)	.35643	.58004	.11321
C (6)	.54654	.45995	.12142

TABLE 5.2

Bond Lengths and their Standard Deviations both (Å)

<u>Bond</u>	<u>Length</u>	<u>e.s.d.</u>
S -C(1)	1.659	0.011
N(1)-C(1)	1.335	0.013
N(2)-C(2)	1.352	0.017
N(2)-C(6)	1.325	0.016
C(2)-C(3)	1.400	0.021
C(1)-C(6)	1.525	0.014
C(3)-C(4)	1.419	0.028
C(4)-C(5)	1.393	0.017
C(5)-C(6)	1.392	0.016

TABLE 5.3Bond Angles and their Standard Deviation

<u>Atoms</u>	<u>Angle</u>	<u>e.s.d.</u>
C(2)-N(2)-C(6)	117.7°	1.1°
N(2)-C(2)-C(3)	122.1	1.6
C(2)-C(3)-C(4)	119.0	1.3
C(3)-C(4)-C(5)	118.2	1.3
C(4)-C(5)-C(6)	117.7	1.3
C(5)-C(6)-N(2)	125.2	1.0
S -C(1)-C(6)	122.3	0.8
S -C(1)-N(1)	124.3	0.8
N(1)-C(1)-C(6)	113.4	1.0
C(1)-C(6)-N(2)	113.5	0.9
C(1)-C(6)-C(5)	121.3	1.1

BOND LENGTHS AND ANGLES IN 2-THIOAMIDO PYRIDINE.

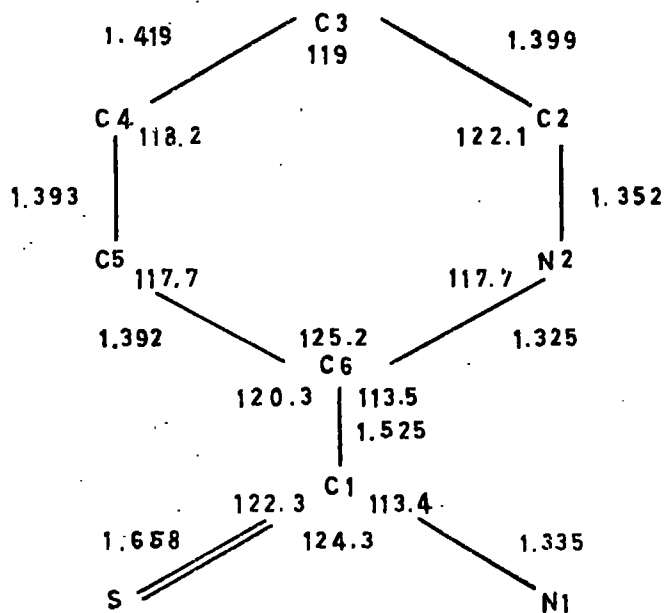


(Fig. 5.2)

BOND LENGTHS AND ANGLES IN PYRIDINE.

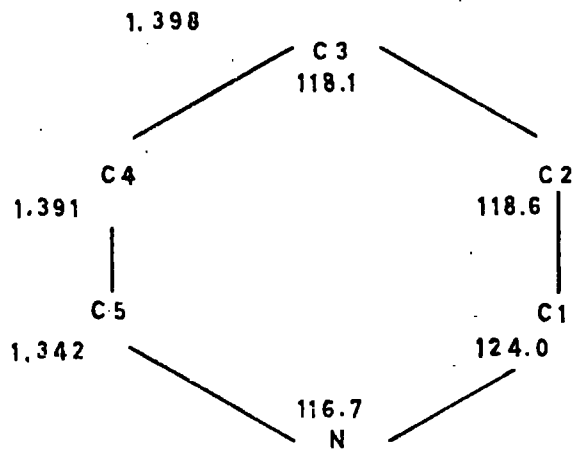


(Fig. 5.3)

CHAPTER SIX

CONCLUSION

6 Conclusion

The bond lengths and angles obtained from the crystal structure analysis of 2-thioamidopyridine show good agreement with similar lengths and angles in related molecules. The intensity record for this analysis was obtained from the Joyce-Loebl integrating microdensitometer. The inference is that the instrument provides a satisfactory intensity record provided certain precautions are taken. The most important single feature of the technique of using the instrument is to limit all measurements to within the linear range of the film employed for the intensity record. Usually the linear range of the film will lie inside the linear range of the instrument. This is the case with ILFORD INDUSTRIAL G, a widely used X-ray film. Experience has shown that it is difficult to estimate visually the intensity of a reflection whose peak density precludes its measurement on the integrating microdensitometer. The tendency is to under estimate. Similarly, it is difficult to estimate visually the intensity of a reflection which is barely visible but is too weak for accurate measurement on the instrument. The tendency here is to overestimate. Usually few reflections occur in either of these categories and the safest procedure is probably to omit them from the intensity record.

The satisfactory nature of the instrument has been further substantiated by at least one known published structure analysis (Ehrenberg, 1967). Consequently, future aims should be directed towards extracting the maximum possible accuracy from the instrument.

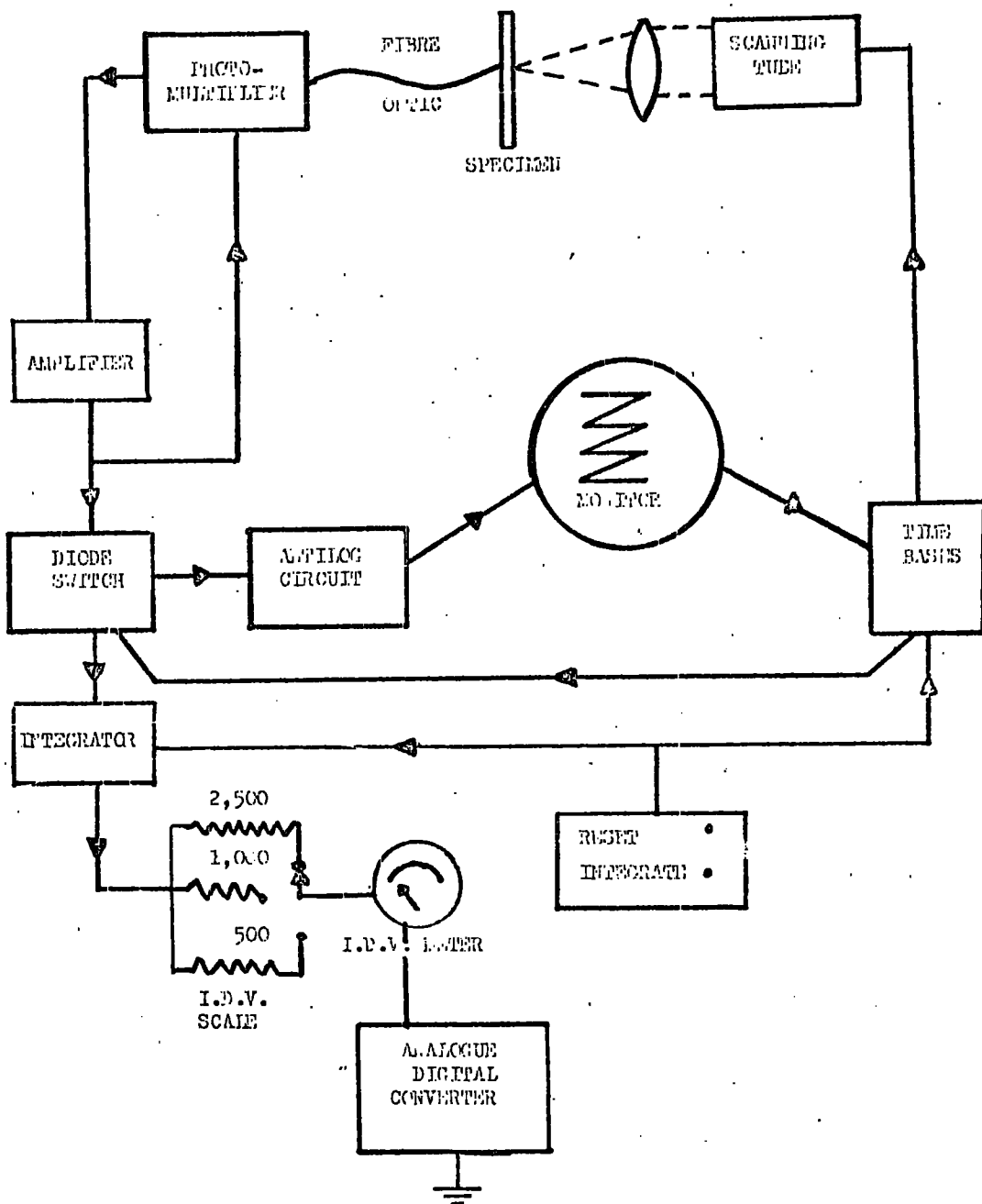
It has already been suggested that the replacement of double with

single coated film could assist in this respect. In addition to this, the size of spot and the associated I.D.V. range should be considered. Large spots i.e. 0.5 mm diameter and above, should be avoided, since the instrument has to be operated at reduced sensitivity in order to accommodate them. Very small spots i.e. 0.2 mm diameter or less, should be avoided because of the usually, very narrow I.D.V. range associated with spots of this size. The optimum size of spot should be such that can be accommodated within X and Y sweep values of three. The maximum I.D.V. associated with this spot size should be about 250 units. It should be possible to achieve these conditions without involving large crystal sizes. In any discussion of crystal size, however, absorption effects will have to be considered.

By careful attention to the details involved it should be possible to obtain from the integrating microdensitometer a reliable and possibly a more accurate intensity record than can be obtained either from a visual estimation or from a photometer of a non-integrating type.

APPENDIX I

JOYCE LOEBL INTEGRATING MICROANALYSIS CIRCUIT DIAGRAM



APPENDIX II

TABULATED RESULTS

Table 3.1

<u>Glass Test Wedge</u>	<u>Photo. Mult.</u>	<u>Instrument</u>
<u>Density</u>	<u>Output Voltage</u>	<u>D Meter Value</u>
0.15	32	0.2
0.26	64	
0.38	90	0.4
0.49	116	
0.60	140	0.6
0.73	170	
0.85	196	0.8
0.99	224	
1.08	244	1.0
1.18	276	
1.29	300	1.2
1.41	324	
1.50	344	1.4
	(380)	(1.6)
	(420)	(1.8)

Table 3.2

Spot	P.D.	X Y 2 2	X Y 3 2	X Y 4 2	X Y 5 2	X Y 2 3	X Y 3 3	X Y 4 3	X Y 5 3
2	0.5	40	40	20	30	50	30	30	20
3	0.5	60	60	50	40	70	70	50	30
5	0.5	120	80	70	70	130	90	70	50
8	0.5	225	150	140	110	220	160	120	90
12	0.5	330	230	180	160	320	240	190	150
16	0.5	430	320	250	200	420	330	260	200
20	0.5	530	400	300	260	540	410	310	240
25	0.5	670	500	380	300	650	500	370	290
30	0.6	770	580	420	340	760	560	430	340
35	0.6	810	640	470	370	820	620	480	370
40	0.7	890	700	530	400	910	690	530	410
45	0.8	1010	780	590	490	1030	760	590	470
50	0.9	1110	820	630	550	1100	830	630	520
60	1.0	1250	990	730	600	1280	940	730	610
80	1.1	1500	1130	890	740	1520	1160	890	730
100	1.2	1500	1280	960	830	1710	1330	1000	830

Table 3.3.

<u>Exposure Time</u>	<u>Spot Intensity (I.D.V.)</u> <u>on same scale as</u> <u>exposure time</u>	<u>Instrument Extinction</u> <u>D Value</u>
2	2.0	↓
3	3.5	
5	5.0	less than
8	10.0	↓
12	13.0	0.5
16	18.0	↓
20	21.5	
25	27.0	0.5
30	30.0	0.6
35	34.0	
40	38.0	0.7
45	43.0	0.8
50	45.0	0.9
60	53.0	1.0
80	63.0	1.1
100	69.0	1.2

Table 3.4

<u>Exposure</u>	<u>I.D.V. (Scaled)</u>	<u>Peak Density</u>	
		(1)	(2)
2	1.3	less	0.05
3	2.6	↓ than	0.07
5	5.0	↓ 0.5	0.16
8	7.6	↓ 	0.40
12	12.5	0.5	0.50
16	16.0	0.6	0.60
20	20.0	0.7	0.70
25	24.0	0.9	
30	26.4	"	
35	27.6	"	
40	31.6	"	

- (1) Density values obtained from the JOYCE-LOEBL integrating microdensitometer (F.S.S.)
- (2) Density values obtained from the JOYCE-LOEBL microdensitometer MK III CS, after scaling to F.S.S. scale.

Table 4.1.1

0.5 mm Collimator

SINGLE COATED FILM

Exposure Time Secs	Y Value	X Value	Determined I.D.V.	I.D.V. X = 3	Peak Density Value
2	2	3	28	28	less
3	2	3	77	77	than
5	2	3	92	92	0.5
8	2	3	127	127	"
12	2	3	201	201	"
16	2	3	268	268	0.5
20	2	3	302	302	"
25	2	3	345	345	0.7
30	3	3	356	356	"
35	3	3	405	405	"
40	3	3	439	439	0.9
45	3	3	469	469	"
50	3	3	492	492	"
60	3	3	564	564	1.0est
70	3	4	464	619	1.1
80	3	4	509	679	"
100	3	4	583	777	1.1
120	3	4	645	860	"
140	3	5	535	888	"
160	3	5	550	917	"
180	3	5	567	945	"
200	3	5	588	980	"
220	3	5	568	947	"
240	3	5	414	690	"
260	3	5	554	923	"
280	3	5	532	887	"
300	3	5	554	923	"
320	3	5	578	963	"
340	3	5	613	1022	"
360	3	5	643	1072	"
380	3	5	648	1080	"

Table 4.1.2

0.5 mm Collimator

DOUBLE COATED FILM

Exposure Time Secs	Y Value	X Value	Determined I.D.V.	I.D.V. X = 3	Peak Density Value
3	3	3	165	165	less than
5	3	3	189	189	0.5
8	3	3	275	275	0.5
12	3	3	428	428	0.9
16	3	3	492	492	1.0est
20	3	4	446	595	1.1
25	3	4	498	664	"
30	3	4	519	692	"
35	3	4	536	715	1.2est
40	3	4	556	741	"
45	3	4	583	777	"
50	3	4	618	824	"
60	3	4	673	897	1.3
70	3	5	577	962	"
80	3	5	594	990	"
90	3	6	556	1112	"
100	3	6	586	1172	"
120	3	6	609	1218	"
140	3	6	644	1288	"
160	3	6	1000	-	"
180	3	6	1000	-	"

Table 4.1.3COMPARISON OF THE I.D.V'S. OF SINGLE AND DOUBLE COATED FILMS

0.5 mm Collimator

Exposure Time Secs	Peak Density		Ratio of I.D.V's. ($\frac{\text{Double Coated}}{\text{Single Coated}}$)
	Single Coated Film	Double Coated Film	
3	less than	less than	2.14
5	0.5 D	0.5 D	2.06
8	↓	0.5	2.15
12	↓	0.9	2.14
16	0.5	"	1.84
20	"	1.1	1.97
25	0.7	"	1.93
30	"	"	1.94
35	"	"	1.76
40	0.9	"	1.69
45	"	"	1.67
50	"	"	1.67
60	"	1.3	1.59
70	1.1	"	1.56
80	"	"	1.46
100	"	"	1.51
120	"	"	1.42
140	"	"	1.46

Table 4.2.1

0.3 mm Collimator

SINGLE COATED FILM

Exposure Time Secs	Y Value	X Value	Determined I.D.V.	I.D.V. X = 3	Peak Density Value
2	3	3	Undetectable	-	less than 0.5
3	3	3	13	13	"
5	3	3	24	24	"
8	3	3	36	36	"
12	3	3	60	60	"
16	3	3	81	81	"
20	3	3	95	95	"
25	3	3	128	128	0.5
30	3	3	150	150	"
35	3	3	170	170	0.7
40	3	3	186	186	"
45	3	3	196	196	"
50	3	3	219	219	0.9
55	3	3	236	236	"
60	3	3	241	241	"
65	3	3	249	249	"
70	3	3	264	264	"
75	3	3	274	274	"
80	3	3	290	290	"
85	3	3	300	300	"
90	3	3	307	307	"
100	3	3	321	321	"
110	3	3	338	338	1.0 est.
120	3	3	353	353	"
130	3	3	378	378	1.1
140	3	3	389	389	"
150	3	3	406	406	"
160	3	3	393	393	"
170	3	3	402	402	"
180	3	3	417	417	"
190	3	3	438	438	"
200	3	3	451	451	"

Table 4.2.2

0.3 mm Collimator

DOUBLE COATED FILM

Exposure Time Secs	Y Value	X Value	Determined I.D.V.	I.D.V. X = 3	Peak Density Value	
					(1)	(2)
2	3	3	13	13	less	0.05
3	3	3	26	26	than	0.07
5	3	3	50	50	0.5	0.16
8	3	3	76	76	"	0.40
12	3	3	125	125	0.5	0.50
16	3	3	160	160	0.6est	0.60
20	3	3	200	200	0.7	0.70
25	3	3	240	240	0.9	
30	3	3	264	264	"	
35	3	3	266	266	"	
40	3	3	316	316	"	
45	3	3	344	344	1.0est	
50	3	3	361	361	"	
55	3	3	380	380	"	
60	3	3	391	391	"	
65	3	3	398	398	"	
70	3	3	365	365	"	
75	3	3	386	386	"	
80	3	3	399	399	"	
85	3	3	413	413	"	
90	3	3	456	456	1.1	
100	3	3	478	478	"	

- (1) These peak density values were obtained from the integrating microdensitometer.
- (2) These peak density values were obtained from the Joyce-Loebl microdensitometer MK III CS, and scaled to the same scale as the integrating microdensitometer density values.

Table 4.2.3

COMPARISON OF THE I.D.V'S. OF SINGLE AND DOUBLE COATED FILMS

0.3 mm Collimator

Exposure Time Secs	Peak Density		Ratio of I.D.V's. (<u>Double Coated</u> <u>Single Coated</u>)
	Single Coated Film	Double Coated Film	
2	less	less	-
3	than	than	2.00
5	0.5	0.5	2.08
8	"	"	2.11
12	"	0.5	2.08
16	"	"	1.98
20	"	0.7	2.10
25	0.5	0.9	1.87
30	"	"	1.76
35	0.7	"	1.57
40	"	"	1.70
45	"	"	1.75
50	0.9	"	1.65
55	"	"	1.61
60	"	"	1.62
65	"	"	1.60
70	"	"	1.29
75	"	"	1.41
80	"	"	1.38
85	"	"	1.37
90	"	1.1	1.48
100	"	"	1.49

Table 4.3.1

0.3 mm Collimator

COMPARISON OF $\frac{\text{I.D.V.}}{\text{EXPOSURE}}$ RATIOSSINGLE COATED FILMDOUBLE COATED FILM

Exposure Time Secs	Peak Density	Ratio $\frac{\text{I.D.V.}}{\text{Exposure}}$	Exposure Time Secs	Peak Density	Ratio $\frac{\text{I.D.V.}}{\text{Exposure}}$
3	less than	4.3	3	less than	8.9
5	0.5	4.8	5	0.5	10.0
8	"	4.5	8	0.5	10.0
12	"	4.8	12	0.5	10.8
16	"	5.1	16	0.6 est	10.0
20	"	4.8	20	0.7	10.0
25	0.5	5.1	25	0.9	9.6
30	"	5.0	30	"	8.8
35	0.7	4.9	35	"	7.6
40	"	4.7	40	"	7.9
45	"	4.4	45	1.0 est	7.6
50	0.9	4.4	50	"	7.2
55	"	4.4	55	"	6.9
60	"	4.3	60	"	6.5
65	"	4.0	65	"	6.1
70	"	3.8	70	"	5.2
75	"	4.0	75	"	5.1
80	"	3.7	80	"	5.0
85	"	3.6	85	"	4.9
90	"	3.5	90	1.1	5.1
100	"	3.2	100	"	4.8
110	1.0 est	3.1			
120	"	2.9			
130	1.1	2.9			
140	"	2.8			
150	"	2.7			
160	"	2.5			
170	"	2.4			
180	"	2.3			
190	"	2.3			
200	"	2.3			

APPENDIX IIIKodak Data Sheet SC-15Prevention of Developer Action on One Side of Double Coated FilmProcedure for Large Films

The film to be processed should be fixed on to a supporting sheet, by means of waterproof adhesive tape, with the unwanted emulsion layer in contact with the sheet. The supporting sheet may be a discarded piece of film or a glass sheet, and should be the same size as, or longer than, the film to be processed. Alternatively, when several sheets of film are to be processed, it may be preferable to tape them together in pairs with the unwanted sides together. The processing procedure is then carried out normally and after the outside layers have been cleaned in the fixer, the sandwich can be separated by stripping off the tape or cutting the films apart. Fixing is then continued until both sides of the film are properly fixed. The film is then washed and dried.

REFERENCES

- Abrahams S.C., (1963), Chem. and Eng. News, ____, 108.
- Abrahams S.C., Alexander L.E., Furnas T.C., Hamilton W.C., Ladell J., Okaya Y., Young R.A. and Zalkin A., (1967), Acta. Cryst., 22, 1.
- Abrahams S.C. and Bernstein J.L., (1965), Acta. Cryst., 18, 926.
- Astbury W.T., (1927), Proc. Roy. Soc. (London) A, 115, 640.
- idem. (1929), Proc. Roy. Soc. (London) A, 123, 575.
- idem. (1929), Trans. Farad. Soc., 25, 1.
- idem. (1929), J. Sci. Instr., 6, 2.
- Bak B., Hansen L. and Rostrup-Anderson J., (1954), J. Chem. Phys., 22, 2013
- Bleeksma J., Kloos G. and di Giovanni H-J., (1948), Phillips Tech. Rev., 10, 1.
- Bragg W.H. and Bragg W.L., (1915), "X-rays and Crystal Structure"
G. Bell and Sons, London.
- Bragg W.H. and Bragg W.L., (1913), Proc. Roy. Soc. (London), A, 88, 428.
- Brentano J.C.M., (1945), J. Opt. Soc. Am., 35, 382.
- Buerger M.J., (1960), "Crystal Structure Analysis", John Wiley, London and New York.
- Bullen G.J., (1953), Acta. Cryst., 6, 825.
- Burbank R.D., (1964), Acta. Cryst., 17, 434.
- idem. (1965), Acta. Cryst., 18, 88.
- Cochran W., (1950), Acta. Cryst., 3, 268.
- Cox E.G. and Shaw W.F.B., (1930), Proc. Roy. Soc. (London), A, 127, 71.
- Critchley J.K. and Jeffrey J.W., (1965), Acta. Cryst., 19, 674.
- Dawton R.H.V.M., (1938), Proc. Phys. Soc. (London), 50, 919.
- Dawton R.H.V.M. and Robertson J.M., (1941), J. Sci. Instr., 18, 126.
- Driffield V.C. and Hunter F., (1890), J. Soc. Chem. Ind., 9, 455.
- Du Pre F.K., (1953), Phillips Res. Rep., 8, 411.
- Eastabrook J.N. and Hughes J.W., (1953), J. Sci. Instr., 30, 317.



- Ehrenberg M., (1967), Acta. Cryst., 22, 482.
- Fasham J.A.L. and Wooster W.A., (1958), J. Sci. Instr., 35, 153.
- Grenville-Wells J., (1955), Acta. Cryst., 8, 512.
- Harding T.T. and Wallwork S.C., (1955), Acta. Cryst., 7, 787.
- Hanic F., (1966), Acta. Cryst., 21, 322.
- Hofstadter R., (1949), Phys. Rev., 75, 796.
- Jeffrey J.W., (1963), J. Sci. Instr., 40, 494.
- Jeffrey J.W. and Rose K.M., (1964), Acta. Cryst., 17, 21.
- idem. (1964), Acta. Cryst., 17, 343.
- idem. (1968), Acta. Cryst., B24, 653.
- Jeffrey J.W. and Whittaker A., (1965), Acta. Cryst., 19, 963.
- Kohler T.R. and Parrish W., (1955), Rev. Sci. Instr., 26, 374.
- Lonsdale K., (1948), Acta. Cryst., 1, 49.
- Lonsdale K., MacGillavry C.H., Milledge H.J., de Wolff P.M. and Parrish W., (1962), "International Tables for X-ray Crystallography, Vol. III", Section 3.1, The Kynoch Press, Birmingham.
- Marshall F H., Coltman J.W. and Hunter L.R., (1947), Rev. Sci. Instr., 18, 504.
- Mees C.E.K., (1952), "The Theory of the Photographic Process" McMillan Co., New York, 1942, revised, 1952.
- Monahan J.E., Schiffer M. and Schiffer J.P., (1967), Acta. Cryst., 22, 322.
- Morimoto A. and Uyeda R., (1963), Acta. Cryst., 16, 1107.
- Nelson J.T. and Ellickson R.T., (1955), J. Opt. Soc. Amer., 45, 984.
- Nordman C.E., Patterson A.L., Weldon A.S. and Supper C.E., (1955), Rev. Sci. Instr., 26, 690.
- Parrat L.G., Hempstead C.F. and Jossem E.L., (1952), Rev. Sci. Instr., 23, 1.

- Parrish W. and Taylor J., (1955), Rev. Sci. Instr., 26, 367.
- Phillips D.C., (1954), Acta. Cryst., 7, 746.
- idem. (1956), Acta. Cryst., 2, 819.
- Paul I., (1966), Private communication.
- Raper, E.S., (1966), Joyce-Loebl Rev., 2, 15.
- Robertson J.M., (1933), Proc. Roy. Soc. (London), A, 140, 79.
- Robinson B.W., (1933), J. Sci. Instr., 10, 233.
- Rossman M.G., (1956), Acta. Cryst., 2, 819.
- Sullivan H.M., (1940), Rev. Sci. Instr., 11, 356.
- Sutton G.J., (1963), Aust. J. Chem., 16, 1137.
- idem. (1966), Aust. J. Chem., 19, 2059.
- Swallow A.G. and Truter M.R., (1960), Proc. Roy. Soc. (London), A, 254, 205.
- Trotter J., (1959), Acta. Cryst., 10, 177.
- Van Horn M.H., (1951), Rev. Sci. Instr., 22, 809.
- Wallwork S.C. and Standley K.J., (1954), Acta. Cryst., 7, 272.
- Whittaker E.J.W., (1953), Acta. Cryst., 6, 218.
- Wiebenga E.H., (1947), Rev. Trav. Chim. Pays-Bas, 66, 746.
- Wiebenga E.H. and Smits D.W., (1950), Acta. Cryst., 3, 256.
- Wiebenga E.H. and Smits D.W., (1956), Acta. Cryst., 2, 520.
- Wood R.G. and Williams G., (1948), J. Sci. Instr., 25, 202.
- Wooster W.A., (1964), Acta. Cryst., 17, 878.

